Archaeologia Baltica 30, 2023, 6–40

Analysis of cultural heritage reference materials by portable and energy dispersive X-ray fluorescence measuring methods: results reliability assessment[1]

Audronė Bliujienė[1],
https://orcid.org/0000-0001-5526-3885
Šarūnas Jatautis[1], Sergej Suzdalev[1, 2] and Gediminas Petrauskas[1*]
https://orcid.org/0000-0002-3328-819X

[1] Klaipėda University, Institute of Baltic Region History and Archaeology, Herkaus Manto St. 84, LT-92294 Klaipėda, Lithuania
[2] Klaipėda University, Marine Research Institute, Universiteto Ave. 17, LT-92294 Klaipėda, Lithuania

Keywords

X-ray fluorescence spectrometry, copper alloys, cultural heritage alloy reference materials, measuring methodology, predictive analytics, results testing

Abstract

This article discusses the results of a large-scale analysis of five cultural heritage alloy reference materials (CHARM) and their shavings using handheld (pXRF) and stationary energy dispersive (ED-XRF) spectrometers. The primary objective of these studies was to assess the capability of the pXRF and ED-XRF spectrometers as a non-invasive surface-measuring technique used for the analysis of the reference materials and the reliability of the data obtained. The second objective was to evaluate the capability of the pXRF and ED-XRF spectrometers used for the analysis of shavings of the same five reference materials and to assess the data obtained. These objectives required finding the best fitting analytical tools for the comparison, and the assessment of the reliability of the data, and, very importantly, finding reliable models for data analysis and results validity verification.

Based on the analysis carried out on the cultural heritage alloy reference materials, it can be concluded that the results of XRF spectrometry obtained from both spectrometers are reliable and can be compared to each other by making reference to four basic conditions: that the provided analysis should be based on certified reference materials of known elemental composition; that analysis be performed according to appropriate measuring methodology (research protocol); that analysing tools (predictive analytics) be clearly defined; and, finally, that testing be done on archaeological artefacts. The reliability and inter-correlation of the results obtained were assessed to determine the possibility of successfully applying XRF spectrometry in the investigation of archaeological artefacts produced from copper alloys.

Introduction

In the first stage of investigation, the authors of this article, being aware of the potential of X-ray fluorescence (XRF) spectrometry, as a surface-measuring method, posed the main research question, which can be formulated as follows: are the certified reference materials (or standards, henceforth CRM) used, and the analytical results obtained by handheld (pXRF) and stationary energy

[1] This article is partly based on freely available research data on reference materials (CHARM). For this see Bliujienė et al. 2023.

* Corresponding author. E-mail: gediminas.petrauskas@gmail.com

DOI: https://dx.doi.org/10.15181/ab.v30i0.2562
Received 17 September 2023; Revised 21 October 2023; Accepted 3 November 2023

dispersive (ED-XRF) spectrometers or analytical devices reliable? To determine the magnitude of the potential bias, we analysed the surface of five cultural heritage alloy reference materials (hereinafter referred to as CHARM[2]) and their drilled shavings. The CHARM set is a group of certified reference materials with a range of compositions similar to that of ancient copper alloys (Heginbotham et al. 2011). The measured composition values of the standards and their shavings were compared with the manufacturer's stated composition values (which in our study were considered to be the correct values), and the measurement bias was determined. The next important issue was the analysis of the standards and their shavings that was carried out to determine the bias and the limits of the measurements made by the pXRF and ED-XRF methods. These CHARM investigations have also provided insight into the potential magnitude of the bias in the analysis of archaeological copper alloys, and how to experimentally match the configuration of the uneven surface of the archaeological finds using shavings of the standard. Even if the surface of an archaeological artefact appears visually relatively flat, a microscopic examination of the find shows that the surface is neither flat nor homogeneous, in fact, the surfaces of the finds are semi-smooth, or uneven.

A further question concerns a very important issue persisting in modern spectrometric analysis of copper alloys, i.e. the possibility of inter-relating investigation results obtained by different spectrometric methods. This issue has been and continues to be raised by many scholars (cf. Carter et al. 1983; Lutz and Pernicka 1996; Bos et al. 2000; Sitko and Zawisza 2005; Heginbotham et al. 2011; 2015; Liritzis and Zacharias 2011; Pollard et al. 2018, pp. 75–76; Lam 2021). Another issue raised is the need for X-ray fluorescence as a non-invasive surface measuring quantitative method as an attempt to find objective ways to assess the best method to compare analyses performed on a flat CHARM standard surface and its shavings (cf. Porcinai et al. 2023). In this way, XRF spectrometry raises the need to investigate possible deviations between the flat CRM surfaces and uneven shavings surfaces. Again, the results of these analyses can be applied to the investigation of real archaeological finds.

In the second stage of our study, a predictive machine learning regression model was developed to adjust the pXRF and ED-XRF spectrometric values of the composition of the CHARM surfaces and their shavings to the known values of the standards and thus to reduce the bias (found in the first stage of the process). The predictive machine learning regression model discussed in this article is a useful theoretical approach to the analysis of archaeological finds.

1. Historiographical overview of surface-based X-ray fluorescence spectrometry

Archaeometrical analysis that began almost 250 years ago with the gravimetric (or the wet chemistry) method continues to this day to be run in different laboratories across Europe. At the same time, it must be acknowledged that the same core issues (characterisation of the alloys, differences with regard to their chronology and geographical setting, the identification of possible sources of raw materials) remain at the heart of already completed and currently ongoing long-term projects. However, the archaeometallurgical research trend that has emerged since the end of the 20th century has been the concept of linking the results of the studies carried out (Carter et al. 1983; Pollard et al. 2018). This concept stems from the need to have the widest possible database of spectrometric studies of copper alloys, covering a much wider area than a single specific region for a given chronological period. It seems that the analysis that is carried out is generating a large amount of closed, seemingly difficult to compare or self-referencing data. As early as the end of the 20th century, different laboratories carried out tests on the same artefacts using different spectrometric methods, allowing the results to be correlated, and demonstrated that modern analytical techniques are capable of producing accurate, reproducible data which, with thorough standardisation, can be used interchangeably with other data and behave similarly in clustering and classification (Northover and Rychner 1998, p. 31; Pollard et al. 2018, pp. 68–70). The development of CHARM is also a consequence of the desire to compare results.

Since the end of the 20th century, XRF has come into play in addressing the issues listed above. XRF can perform multi-element analysis simultaneously and is a rapid and non-invasive surface-measuring method. XRF can investigate archaeological finds, but its weakness is the significant spectral overlap and results reliability depending on the degree of surface preparation and the fit of the test object to the bench of the research area, usage of appropriate standards, and calibration methods used (Lutz and Pernicka 1996; Bayley and Butcher 2004, pp. 14–22; Pollard et al. 2018, pp. 63–64, 77–78, Table 1). Therefore, in modern archaeometallurgical research and results evaluation, as well as in assessments of the reliability and reproducibility of survey results, it is recommended that a sufficient number of standards be used. However, the scientific literature is divided on the number of standards needed to ensure the reliability of the results obtained (Injuk et al. 2006,

[2] These reference materials or standards are numbered according to their acquisition time in the project 'Copper alloys in the first millennium AD: Investigations of metallurgy and technological processes in the context of socio-economic development'. The specification of the CHARM standards given in the text and in Tables 1 and 2.

p. 429; Shackley 2010; Heginbotham et al. 2011, 2015; Pollard et al. 2018). The authors of this article carried out a reliability assessment of five CHARM and their drilled shavings. The results of the analysis show that not only the number of standards but also their suitability for archaeological investigations of copper alloys is very important because it has a huge impact on determination of the reliability of the analysis performed (Mantler et al. 2006, p. 326; Shackley 2010, 2011; Shugar 2013; Speakman and Shackley 2013; Pollard et al. 2018, pp. 75–76; Roxburgh 2019). It is also important to note the biases encountered by all researchers attempting to correlate the values of any standard for copper alloys with their own analysis (Roxburgh 2019, Figs. 1 and 2; Roxburgh et al. 2019; Lam 2021; Steenstra et al. 2022).

Another problem with both pXRF and ED-XRF methods is the inherent issue of the reliability of X-ray fluorescence spectrometry itself as a surface measuring technique. As early as 1995, handheld or portable X-ray fluorescence spectrometers (pXRF) became popular and underwent rapid technological development. Thus, lightweight handheld X-ray fluorescence spectrometers were adapted to work both in field conditions and in museum storage, and, of course, in laboratories (Frahm and Doonan 2013; Shugar 2013; Pollard et al. 2018, pp. 63–64, Table 1; Roxburgh 2019; Roxburgh et al. 2019). Nevertheless, a discussion arose in the scientific press highlighting the weaknesses of the pXRF method and the reliability of the data obtained by this spectrometric technique. The main issues raised in the discussion were the capabilities of these analytical devices and whether it is possible to obtain reliable results measuring corroded (or patina) layers of archeological finds with different configuration and surface reliefs (Lutz and Pernicka 1996; Gigante et al. 2005; Shackley 2010, 2011; Liritzis and Zacharias 2011; Frahm 2013a, 2013b; Shugar 2013; Speakman and Shackley 2013; Ferretti 2014; Pollard et al. 2018, pp. 75–76; also see Roxburgh 2019). The recent FLAME (Flow of Ancient Metal across Eurasia) research project (Pollard et al. 2018) has once again drawn attention to the debate that arose a decade ago, claiming that the reliability of XRF spectrometric analysis is an issue, in particular with regard to the reliability of the pXRF results, although it is claimed that the results 'may be usable *in extremis* for allocation to alloy types, although subject to considerable uncertainty' (Pollard et al. 2018, pp. 62–63). However, by applying proposed methodologies, it has been possible to identify alloy types for both the CRM and the archaeological finds. One of the most widely used methods to determine the types of archaeological finds was proposed by Bayley and Butcher (2004, pp. 22–25, Figs. 5–8, Table 5).[3] At the same time, it should be noted that the chemical analysis of many archaeological finds does not correspond to modern definitions of alloys. One of the reasons for this phenomenon is the fact that archaeological finds contain main copper alloying elements (zinc, tin and lead) either below or higher than any scientifically estimated levels or levels that would be expected if the sole source for making copper alloy was direct copper ore sources. On the other hand, studies on copper alloys, ranging from gravimetry methodology to recent advanced spectrometric analysis, can prove that chronological changes in copper alloy types in central and northeastern Europe followed a similar rhythm during the whole of the 1st millennium AD (Bezzenberger 1904, p. XVIII; Vaitkunskienė and Merkevičius 1978; Jouttijärvi 2017; Roxburgh and Olli 2018; Roxburgh 2019; Roxburgh et al. 2019; Bliujienė et al. 2021b).

Therefore, it should once again be noted that X-ray spectrometry faces fundamental problems as a non-invasive surface-measuring method. That is why, above all, it is most important to address research questions properly formulated within the limits of the X-ray spectrometry as a semi-quantitative spectrometric method, which enable the categorisation of copper alloys into types according to the main alloying elements, and this is a very significant result. However, discussion that took place did not underestimate X-ray spectrometry and handheld devices as working tools, but simply confirmed the well-known truth that the spectrometric technology can be successfully applied by understanding the limits of its application — the determination of the types of copper alloys, in other words the metallurgically based characteristic of alloying metals at presence/absence at ± 1% (Pollard et al. 2018, pp. 115–118, Table 1).

X-ray spectrometry and handheld spectrometers, like stationary ones, open the door to the categorisation of copper alloys from archaeological finds into types (brass, leaded brass, bronze, leaded bronze, gun metal, leaded gun metal, and leaded copper) (Bayley and Butcher 2004, pp. 22–24, Figs. 6–8; Pollard et al. 2018, p. 117, Table 1; Roxburgh 2019, pp. 34–35, Figs. 1 and 2; Bliujienė et al. 2023). Obviously, this also opens another door, namely to the types of copper alloys that have been identified, allowing us to perform comparative analysis with published data and other datasets that have already been compiled.

2. Materials

In this article, we present the results of the pXRF and ED-XRF analysis of the five CHARM and their drilled shavings. In total, 1,502 individual measurements of CHARM

[3] It must be acknowledged that metallurgical studies have applied, and continue to apply, slightly different criteria for categorising copper alloys into types. However, Zn, Sn and Pb remain the main copper alloying elements. The ratios of nickel (Ni) to silver (Ag) and of arsenic (As) to antimony (Sb) are also important criteria for the definition of copper alloys (Riederer 1984; Pollard et al. 2015; Pollard et al. 2018).

and 207 individual measurements of shavings were made by both spectrometers and the analytical results reliability assessment was performed (the data are given in Table 1). These data are from the research project 'Copper alloys in the first millennium AD: Investigations of metallurgy and technological processes in the context of socio-economic development'. In the framework of this project, besides CHARM and their drilled shavings, 2,440 archaeological finds from 284 sites were also analysed and are included in the open access database (Bliujienė et al. 2023).

The CHARM set of reference materials is designed for the analysis of copper alloys, specifically for the calibration and harmonisation of the obtained results of XRF spectrometry. In our case, the authors of this article were seeking to harmonise the results obtained by pXRF with ED-XRF results. The CRM set used by us has certified values for Cu, Zn, Sn, Pb, Fe, Ni, As, Ag and Sb, plus S, Cr, Co, Se, Cd, Au, Bi elements. For these CRM, measurements of lead, zinc and tin compared with the reference values and 95% confidence in interval (CI) range (Heginbotham et al. 2011, 2015; Heginbotham and Solé 2017; Heginbotham 2018) have been carried out. A CHARM set in the form of discs manufactured by chill casting, as stated by the producer, was used (https://www.armi.com/en/mbh-now-armi-mbh). For the present research, the following set was analysed: the bronze alloy (32X SN6.B), leaded brass (31X 78359.B), brass alloy (31X TB5.B), gunmetal (33X GM21.B), and leaded bronze (32X LB10.G) (for the values of the elements provided by the producer see Table 2).

3. Methods and analytical tools

XRF analysis using handheld Niton XL3t spectrometer was undertaken (power 2 W, voltage — 50kV, detector area ~ 50 mm^2, calibration mode 'General Metals'). The test bench research area covers the 8 mm spot, the depth of measurement for most elements was restricted to below 0.1 μm, the optimal thickness for XRF is >2 mm. A series of experiments measuring 30 and 60 seconds were carried out on the standards. The results cease to vary within 30 seconds. Therefore, this reading time was deemed sufficient for the present study. In the course of the research, each investigated point was automatically photographed and the spectra lines were recorded, enabling checking of records individually for inconsistencies and unexpected overlaps (Fig. 1). By application of the fundamental parameters (FP), correction method one assumes that all analysed elements add up to 100%. Copper alloys were characterised according to their principal alloying elements (Zn, Sn and Pb) and the presence of small amounts of the deliberately added alloying elements. Values of all elements are given in wt%.

The ED-XRF analysis was carried out in Klaipėda University Marine Research Institute using spectrometer SPECTRO XEPOS HE (power 50 W, electric voltage up to 60kV, detector area 20–30 mm^2), employing the 'FP alloy F(A)' calibration module from the TurboQuant II (TQ) calibration method elaborated by the manufacturers. Each standard was placed in the sample chamber of the device using

Table 1. Empirical reference materials (CHARM) data distribution by type (solid CRM surface and drilled samples or shavings), investigated by pXRF and ED-XRF devisers. Prepared by Bliujienė.

CRM	Type	pXRF	ED-XRF	Total	pXRF	ED-XRF
					%	%
32X SN6.B=1-CHARM	Solid	286	55	341	10.64	2.05
31X 78359.B=2-CHARM	Solid	263	81	344	9.78	3.01
31X TB5.B=3-CHARM	Solid	288	63	351	10.71	2.34
33X GM21.B=8-CHARM	Solid	196	49	245	7.29	1.82
32X LB10.G=9-CHARM	Solid	180	41	221	6.69	1.52
Total		**1213**	**289**	**1502**	**45.11**	**10.74**
CRM	**Type**	**pXRF**	**ED-XRF**	**Total**	**pXRF**	**ED-XRF**
					%	%
32X SN6.B=1-CHARM	Shavings	18	21	39	0.67	0.78
31X 78359.B=2-CHARM	Shavings	18	22	40	0.67	0.82
31X TB5.B=3-CHARM	Shavings	21	22	43	0.78	0.82
33X GM21.B=8-CHARM	Shavings	21	23	44	0.78	0.86
32X LB10.G=9-CHARM	Shavings	18	23	41	0.67	0.86
Total		**96**	**111**	**207**	**3.57**	**4.14**

Table 2. Certified reference materials information for optical emission and X-ray fluorescence devisers. For lead (Pb), zinc (Zn) and tin (Sn), and the main alloying elements compared with the reference values. Value: the certified values are the present best estimates of the true content for each element. Each value is a panel consensus, based on the averaged results of an interlaboratory testing programme. Uncertainty: the uncertainties are generated from the 95% confidence interval derived from the wet analysis result in combination with a statistical assessment of the homogeneity data.

32X SN6.B=1 CHARM	**Bronze alloy**	Cu	Zn	Sn	Pb	Fe	Ni	Ag	Sb	As	Bi	Co	Mn	Au	Cd
CRM (value)		85.73	2	6.78	1.644	0.376	0.295	1.007	0.304	0.804	0.127	0.75	0.09	0.0027	0.0242
Uncertainly		0.1	0.03	0.04	0.012	0.009	0.002	0.013	0.003	0.01	0.003	0.008	0.002	0.0002	0.0007
31X 78359.B=2 CHARM	**Leaded brass**	Cu	Zn	Sn	Pb	Fe	Ni	Ag	Sb	As	Bi	Co	Mn	Au	Cd
CRM (value)		76.6	16.26	1.6	1.045	0.191	0.196	2.014	0.44	0.101	0.91	0.113	0.0045		0.0586
Uncertainly		0.2	0.09	0.02	0.009	0.004	0.003	0.019	0.02	0.004	0.02	0.002	0.0002		0.0015
31X TB5.B=3 CHARM	**Brass alloy**	Cu	Zn	Sn	Pb	Fe	Ni	Ag	Sb	As	Bi	Co	Mn	Au	Cd
CRM (value)		61.49	35.62	0.129	0.575	0.094	0.106	0.216	0.229	0.396	0.292	0.0202	0.283		0.49
Uncertainly		0.07	0.12	0.002	0.008	0.002	0.002	0.003	0.005	0.007	0.008	0.0006	0.005		0.001
33X GM21.B=8 CHARM	**Gunmetal**	Cu	Zn	Sn	Pb	Fe	Ni	Ag	Sb	As	Bi	Co	Mn	Au	Cd
CRM (value) (value)		78.86	4.96	4.5	7.53	0.693	0.197	0.701	1.033	0.333	0.459				0.249
Uncertainly		0.11	0.04	0.06	0.12	0.013	0.004	0.011	0.016	0.004	0.007				0.004
32X LB10.G=9 CHARM	**Leaded bronze**	Cu	Zn	Sn	Pb	Fe	Ni	Ag	Sb	As	Bi	Co	Mn	Au	Cd
CRM (value)		77.1	0.11	8.29	12.6	0.0011	0.69	0.0686	0.599	0.169	0.093	0.084			
Uncertainly		0.16	0.005	0.05	0.13	0.0002	0.008	0.0016	0.008	0.004	0.002	0.002			

Value: the certified values are the present best estimates of the true content for each element. Each value is a panel consensus, based on the averaged results of an interlaboratory testing programme. Uncertainly: the uncertainty are generated from the 95% confidence interval derived from the wet analysis result in combination with a statistical assessment of the homogeneity data.

the sample holders and irradiated for approximately 6 minutes. The TQ method combines different procedures: calculation of the mass attenuation coefficient using the extended Compton model, and the final calibration based on fundamental parameters (FP) procedure in order to convert the original X-ray counts into elemental percentages. The raw data captured at the time of measurement results in a spectrum which is stored separately in the sample file. A spectrum is visualised as a chart of an energy region in correlation to a number of counts recorded by the detection electronics at specific energy values. Values of all elements are given in wt% (Hoffmann, 2006, pp. 770–771; https://extranet.spectro.com/-/media/965AF85D-1942-435E-ABE5-437084E0435D.pdf).

The CHARMs were sampled by drilling with a Proxxon D-54518 Nierstblach electric drill and bits with a diameter of 1.5–2 mm. The homogeneity of the CHARM discs was very important when taking samples by drilling. The shavings of the standards were obtained by drilling the discs laterally at 5 mm from the top surface and then up to 10 mm thickness, and prepared as samples weighing 0.5 g (Fig. 2). The drilled samples in the form of shavings were transferred into 20 mm sample cups, the bottoms of which were covered by protective 4 µm polypropylene foil.

The CHARM standards and shavings were measured by both spectrometers using the same discussed appropriate methodology relevant to the non-invasive surface analysis. This methodology was also used for archaeological artefacts analysis. The analysis of standards by pXRF analysis and stationary spectrometer for ED-XRF strictly followed the established methodology (analytical protocol): all standards used in the studies were analysed at the start

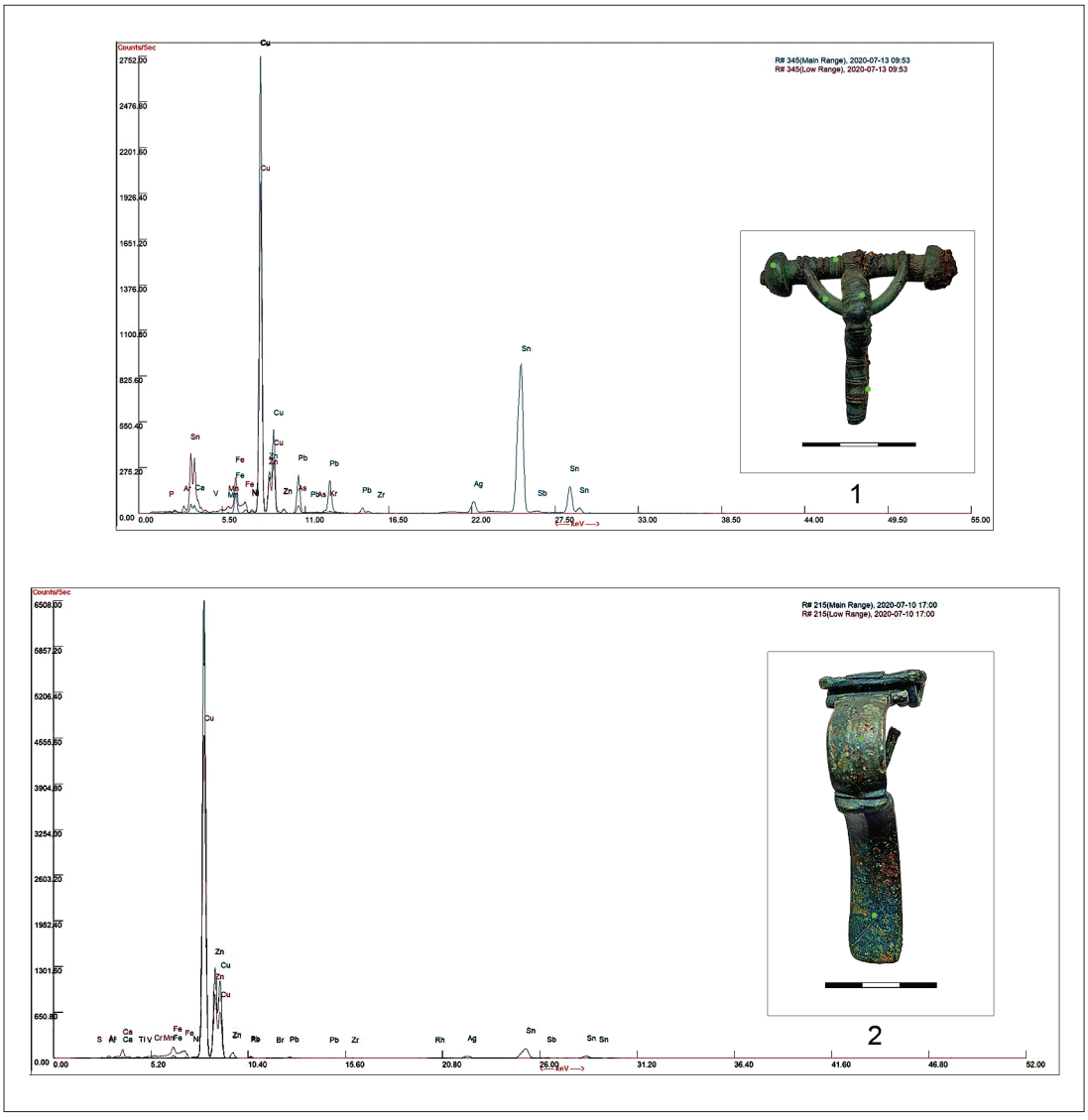

Figure 1. Spectral lines recorded by pXRF for late 1st – late 5th century AD brooches:1. Crossbow brooch with a long foot, found in the first deposit of the Kukiai-Petreliai cemetery (Mažeikiai district; MM GEK 4536); 2. Eye brooch, found in the Zastaučiai barrow cemetery, barrow 2, grave 1 (Mažeikiai district; MM GEK 4536). Photographs by Bliujienė.

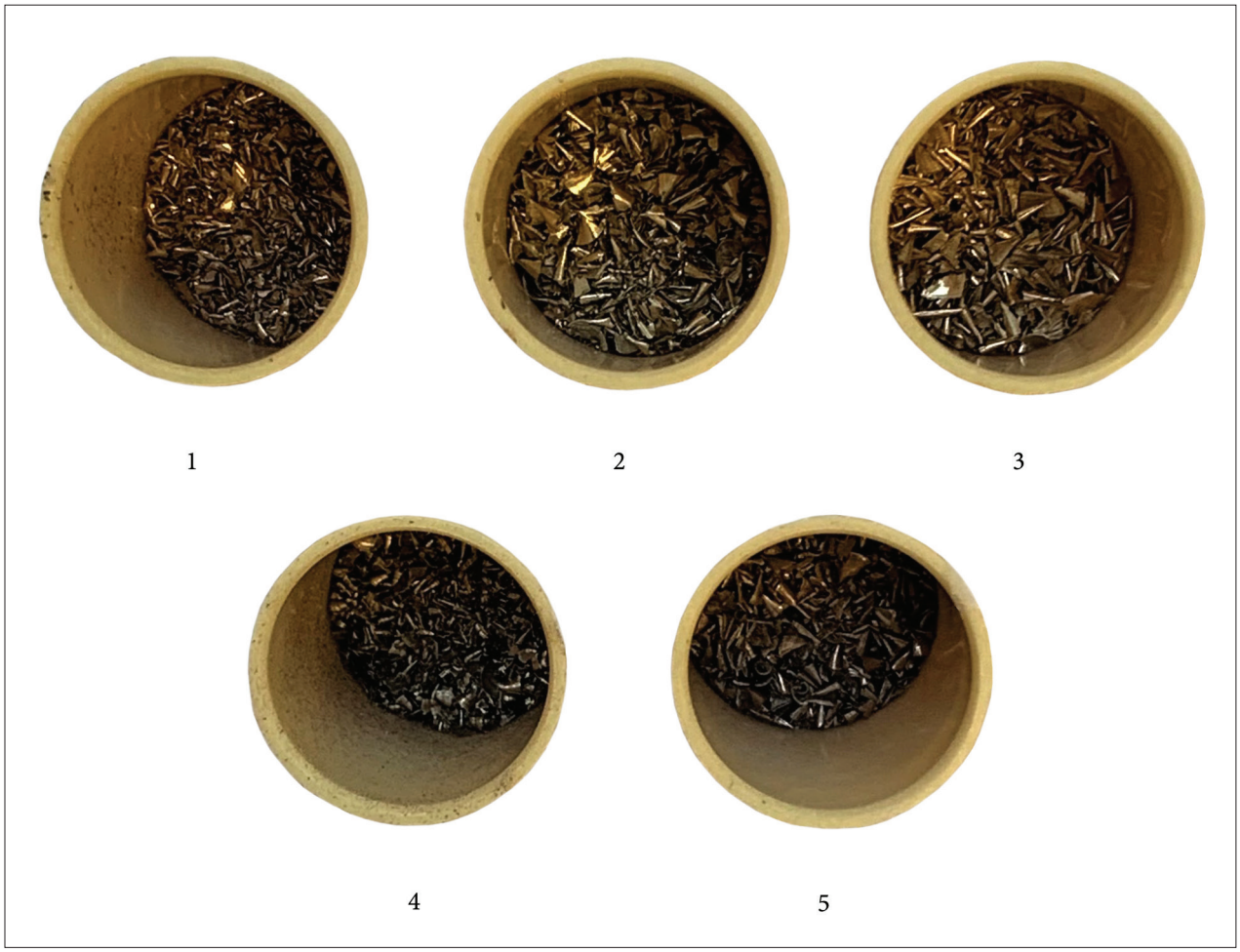

Figure 2. CHARM reference material shavings (samples) in containers covered with two special thin films: 1. Bronze alloy; 2. Leaded brass; 3. Brass alloy; 4. Gunmetal; 5. Leaded bronze. See Table 2 for a description of the reference materials and values. Photograph by Bliujienė.

of each study, at the mid-point and at the end of the fixed study time. This analytical protocol was validated for the studies, as the measurements of all the standards made every two hours consistently showed the same results. The surfaces of the standards to be tested were cleaned with a soft cloth using isopropanol (isopropyl alcohol).

The following standard measures of central tendency were used for descriptive statistics of the data: mean, median, mean absolute difference, median absolute difference, mean absolute percentage difference, and median absolute percentage difference. The following measures of variation were used for hypothesis testing: the length of 95% confidence intervals, first and third quartiles, and interquartile range (the results of these studies are indicated in Appendix 1). Spearman's rank correlation coefficient was used to describe the magnitude of correlation between bivariate data. Euclidean distance was used to quantify differences between multivariate data. Hotelling's T-square test for one sample was used to test the null hypothesis that the differences between obtained pXRF and ED-XRF measurements and standard values are only due to random noise. The XGBoost regression model was chosen to create an adjustment algorithm to predict the 'correct' measurement values given to the obtained pXRF or ED-XRF measurement results (for the values of the standards' surfaces and/or drilled shavings measurements).

In this article, all statistical calculations and graphs were created with Python (version 3.9.13) and R (version 4.2.0). The Pandas, Numpy and Scipy Python libraries were used for the descriptive statistics calculations. The Plotly Python library was used to create the graphs. The XGBoost and Sklearn Python library were used to build machine learning regression models. The DescTools R library was used to estimate results of the Hotellings T-square test (https://cran.r-project.org/web/packages/DescTools/DescTools.pdf; https://numpy.org/; https://pandas.pydata.org/; https://plotly.com/; https://www.python.org/; https://www.r-project.org/; https://scikit-learn.org/stable/; https://scipy.org/; https://xgboost.readthedocs.io/).

4. Results and discussion

In our studies, in total, 1,213 individual measurements of the CHARM standards as the reference materials for bronze alloy, leaded brass, brass alloy, gunmetal and leaded bronze were analysed by pXRF and 289 individual measurements of standards were researched by the ED-XRF method. In addition to this, 96 samples of shavings of these CHARM standards were investigated by pXRF, while 111 samples were determined by ED-XRF (Table 1). The CHARM analysis performed with both spectrometers certainly assessed the reliability of the data from each descriptive statistics method (Appendix 1). These data allow a few key observations to be made about the investigated CHARM standards.

Firstly, higher and lower trends in metal proportions in alloys might be identified by pXRF and ED-XRF spectrometers respectively (Fig. 3). The Spearman rho correlation coefficient values for the CHARM standards obtained by pXRF and ED-XRF spectrometry are positive and high, except for the lower correlation coefficient values for cobalt. Arsenic was not measured by the pXRF spectrometer. High correlation coefficient values indicate that common trends in the composition of different standards are identified by both spectrometers.

Secondly, the bias, still exists (see Appendix 1). That is, the percentage values of the pXRF and ED-XRF measurements are quite significantly different from the reported mean values of the standard. However, this quite significant bias is in line with the capabilities of XRF spectrometry itself. The results of Hotelling's T-square for one sample test (Table 3) suggest that there is evidence to reject the null hypothesis: the observed difference cannot be explained by chance alone. Thus, the analysis of the results shows that appropriate analytical tools, which correctly identify the trend in the distribution of the measurements, have been chosen, while the absolute values are subject to bias.

Thirdly, a more detailed comparison of the differences between the values and the reported CHARM values point to the following main observations. The pXRF measurements are noticeably more accurate and less variable compared to the values obtained by ED-XRF spectrometer. This discrepancy can be clearly seen in reported figures and tables (Fig. 3; Appendix 1).

Fourthly, the bias of the drilled shavings tests is significantly higher compared to the reference surface. This conclusion is valid for the pXRF and ED-XRF drilled shavings test results. In this case, too, the pXRF results are more accurate (Figs. 4 and 5). The analysis carried out made it

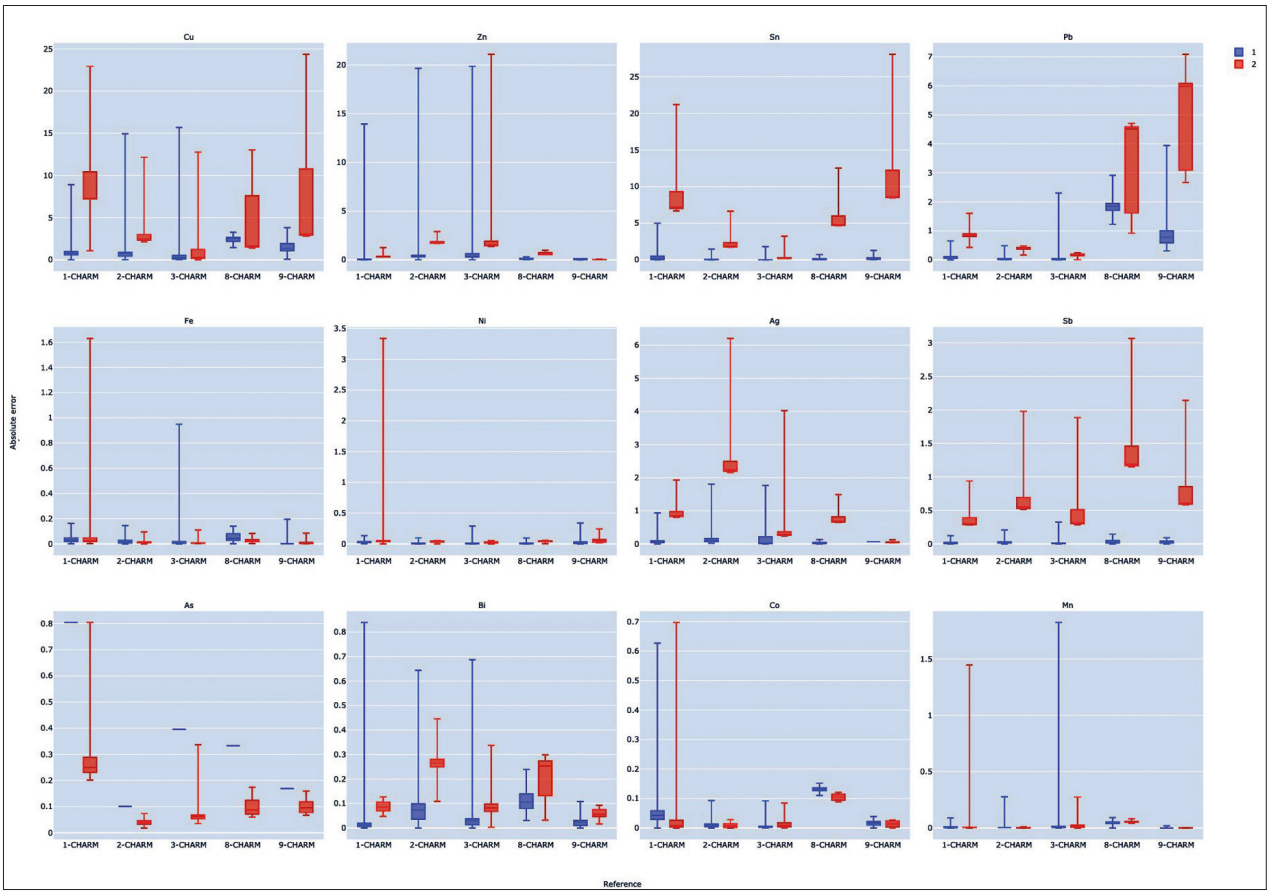

Figure 3. Variation of absolute error: absolute difference between pXRF (1) and ED-XRF(2) values. Outliers (values higher than abs ± 1.5 IQR) were removed. Blue square – pXRF data; red square – ED-XRF data. Prepared by Jatautis.

Table 3. Hotteling's T2 for one sample results are used to statistically assess whether the difference between the measurements and the mean standards is due to random noise. Prepared by Jatautis.

Method	Reference	Hotelling's T2	df1	df2	p-value
pXRF	1-CHARM	16193.76	11	275	< 0.000
pXRF	2-CHARM	2192.84	11	252	< 0.000
pXRF	3-CHARM	425.11	11	277	< 0.000
pXRF	8-CHARM	16178.87	11	185	< 0.000
pXRF	9-CHARM	2576.97	10	170	< 0.000
ED-XRF	1-CHARM	103844.3	12	43	< 0.000
ED-XRF	2-CHARM	175835.78	12	69	< 0.000
ED-XRF	3-CHARM	27275.15	12	51	< 0.000
ED-XRF	8-CHARM	159099.86	12	37	< 0.000
ED-XRF	9-CHARM	216986.09	12	29	< 0.000

possible to conclude that the best agreement was found with the first, second and third CHARM standards. However, this observation is only valid for the pXRF measurements as the biases for ED-XRF are larger. The pXRF measurements (see Appendix 1) served as the basis for the choice of further analysis of the mentioned CHARM standards due to higher precision and lower variation.

The drilled CHARM shavings were analysed by both spectrometers to confirm two scientific hypotheses. Clearly, the first objective was to establish elemental composition. This analysis shows a greater discrepancy between the data obtained by ED-XRF and known CHARM values given the uneven surface of the shavings. In addition, the surface of the drilled samples themselves was not uniformly uneven and consisted of larger and finer pieces of shavings (Fig. 2).

The analysis of uneven shaving surfaces provided an answer to the second hypothesis raised in the article, namely, that the uneven surface of archaeological finds is the result of the manufacturing process (casting, forging or casting and forging) and the decoration of the surface (stamping, carving, engraving, etc.). The unevenness of the surface of archaeological artefacts is exacerbated by the patina formed during the corrosion process and its thickness. Therefore, smooth surfaces such as those observed in the

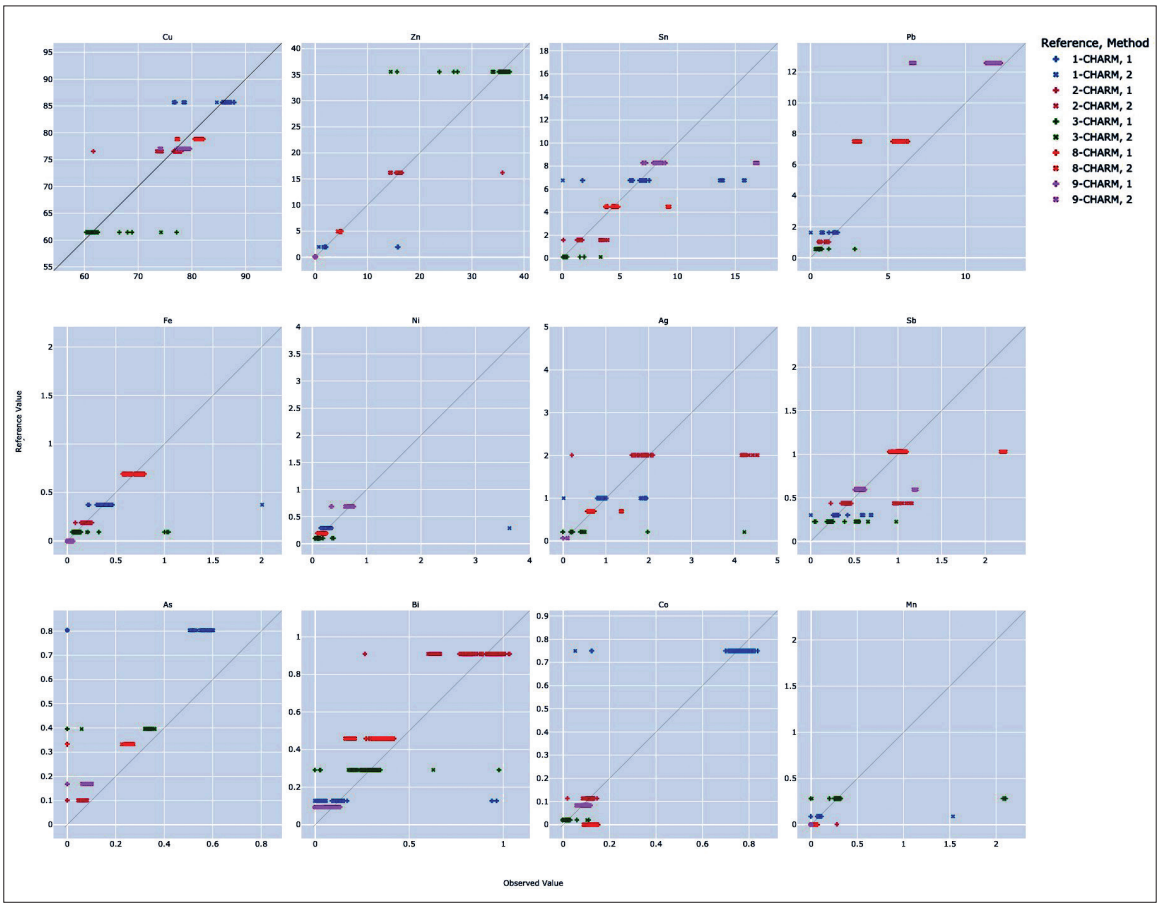

Figure 4. CHARM elements' values versus measured by pXRF (1) and ED-XRF (2) devisers. The grey diagonal line shows where the points should ideally be located if the standard values, and the measurements coincide. pXRF values (1) are marked by sign +; ED-XRF (2) are marked by sing +. Prepared by Jatautis.

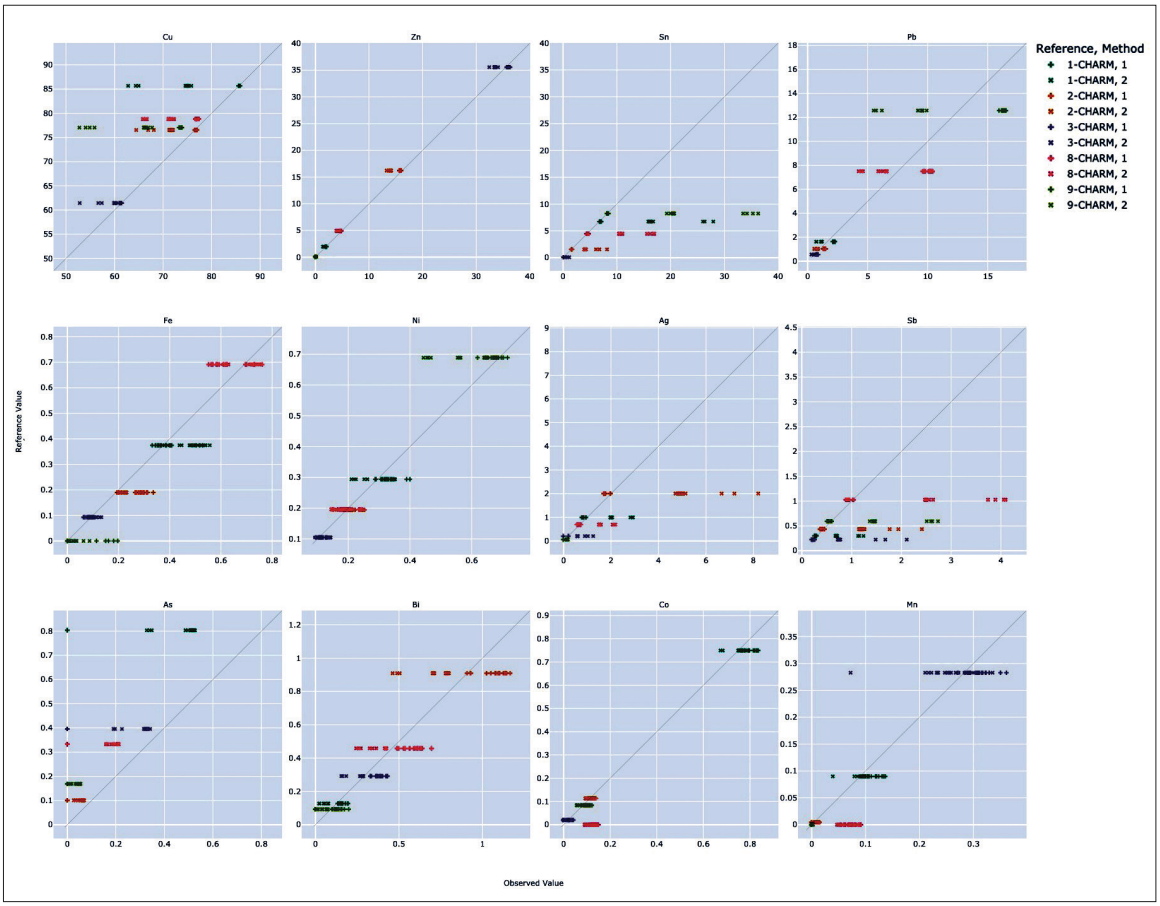

Figure 5. CHARM drilled shavings elements' values versus measured by pXRF (1) and ED-XRF (2) devisers. The grey diagonal line shows where the points should ideally be located if the drilled sample values and the measurements coincide. pXRF values (1) are marked by sign +; ED-XRF (2) are marked by sign +. Prepared by Jatautis.

analysis of the surfaces of the CRM simply cannot exist in the case of archaeological finds (Fig. 6). Yet it is known that on archaeological finds, the ratio of Cu, Zn, Sn and Pb in stages of patina formation is not constant and belongs to the chemical, physical processes that were happening in the soil. The zinc decline in the patina mostly happens after the cementation process, during remelting and reusing of copper alloys (Dungworth 1997, p. 907; Rehren 1999, p. 252; Fernandes et al. 2013; Pollard 2015). Therefore, it is claimed that zinc in the patina can be half as much as in the metal core. However, due to the sequence of corrosion processes, the patina contains a higher concentration of tin and lead (1.8 and 2.6 times, respectively) (Lutz, 1998, p. 170).[4] However, within the limits of the X-ray fluorescence as a semi-quantitative method, the data obtained allows archaeological finds to be classified into copper alloy types (Bayley & Butcher 2004, p. 14, Table 5; Van der Meulen-van der Veen, 2023; Roxburgh et al. 2018, 63, Fig. 2; Roxburgh 2023 b, Fig. 2). Furthermore, using CHARM standards as the reference material is advisable to ensure that as many extraneous factors as possible may be eliminated from the interpretation of important patterns in the dataset (cf. Bliujienė et al. 2023).

The XGBoost prediction model was created to convert the measurement values obtained by both spectrometers into the reference values by minimising the differences between the obtained values of standards and the values given by the producer. The XGBoost prediction model we use is such that, given the pXRF and ED-XRF as methods and the reference material (measured standard surface or drilled shavings), the adjusted values will be obtained from the created prediction algorithm. Analysing the collected data, the best agreement is found for the first, second and third CHARM standards. These are brass alloy (3-CHARM), leaded brass (2-CHARM) and bronze alloy (1-CHARM). These copper alloys were common in different proportions during the 1st millennium AD according to the results of optical emission spectrometry (OES) carried out as early as the 1970s (Vaitkunskienė and Merkevičius 1978, Table 1). The eighth CHARM (gunmetal) and the ninth CHARM (leaded bronze) measurements are characterised by greater variation (Figs. 3–5). It is worth mentioning that in the framework of the large-scale surveys of the archaeological finds of the 1st millennium

[4] However, this conclusion is based on research material from the Roman period.

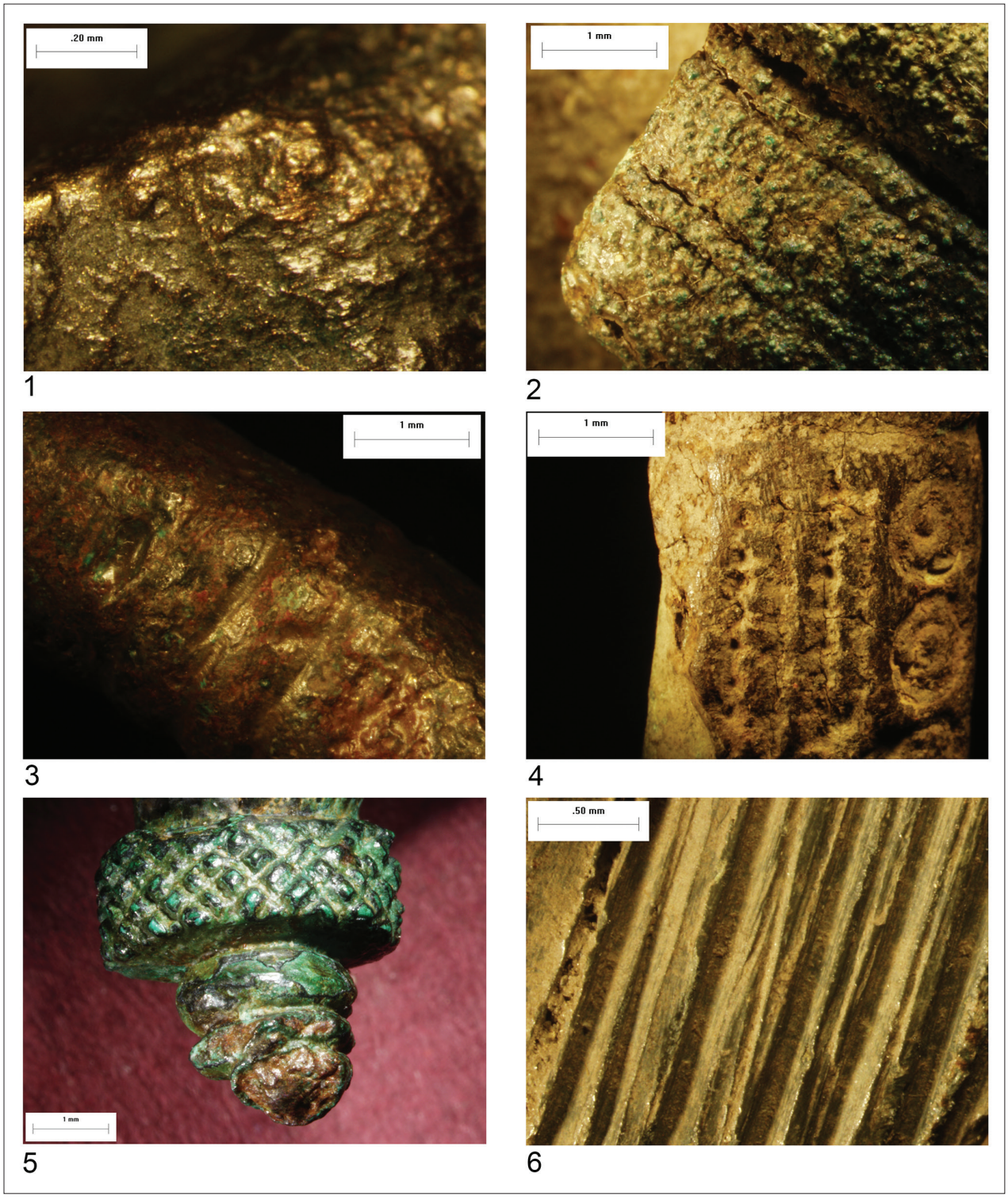

Figure 5. Enlarged ornamented surfaces of the jewellery analysed.
1. Bandužiai (Klaipėda city), sestertius of Emperor Trajan (98–117), grave 24 (MLIM GEK 80098/); 2. Tautušiai (Raseiniai district) brooch of Almgren Type 133, stray find (LNM AR); 3. Paragaudis (Šilalė district), neck-ring barrow II, grave 1 (LNM AR 721: 5); 4. Mačeliai (Akmenė district), bracelet, stray find (LNM Man.1); 5. Barzūnai (Pagėgiai municipality), brooch close to Almgren Type 110, grave 16 (LNM GRD 108822: 133); 6. Florencija (Raseiniai district) brooch of Almgren Type 133, stray find (LNM Fli. 1). Enlarges photographs by Tomas Rimkus. Photographs of artefacts are available from Bliujienė et al. 2023, online database http://lydiniai.lt/.

AD, the results clearly show a greater variety of copper alloy types, allowing the distinguishing of brass-based (brass/gunmetal, leaded brass, leaded brass/gunmetal), gunmetal, and bronzes-based alloys (bronze/gunmetal, leaded bronze/gunmetal, leaded bronze, leaded gunmetal) (Bliujienė et al. 2021a, 2021b; Bliujienė et al. 2023). The variety of brass-based, gunmetal and bronze-based alloys means copper alloys were constantly remelted, mixed and reused (Pollard et al. 2015; Jouttijärvi 2017). Variations in the measurements of the ninth CHARM (leaded bronze) in archaeological finds may be related to the problems of corrosion processes and of alloy homogeneity, that is, the unequal distribution of lead in the alloys (Oudbashi et al. 2013; Roxburgh 2019, pp. 34–35). Hence, XRF spectrometry enables the categorisation of copper alloys into types according to the main alloying elements — zinc, tin and lead.

As mentioned above, the biases in the drilled shavings analysis are significantly higher compared to the CHARM disc solid surface tests, which is true for the pXRF and ED-XRF results (Fig. 5). The surface of the drilled shavings is similar in texture and appearance to the uneven surface of the archaeological finds due to ornamentation or mechanical surface damage. As the shavings from standards of known composition are investigated, the difference in results between the smooth surface of the standard and the roughened surface of the shavings experimentally replicates the situation between the surface of the find and the surface of the reference material. This difference can be calculated by applying empirical and theoretical coefficients, attempting to reduce the variables in order to make the mathematical calculations manageable. These investigations will enable the results obtained to be compared and used in X-ray studies of archaeological finds. These observations are valuable for evaluating XRF results and verifying them with the results obtained from other spectrometric methods. However, our analysis shows that no consistent variation of elemental abundances was observed from rim-to-core along the horizontal section of each drilled standard at least to the depth of about 1 cm. This suggests there is not a large difference in compositional zoning within the CHARM standards used as reference materials, as has already been mentioned by Arlen Heginbotham (2018, pp. 50–62) and Edgar S. Steenstra et al. (2022).

The results discussed in this article could allow researchers to compare the results of the analysis and to replicate this study or carry out further research, as well as develop more accurate correction methods, but also, most importantly, to apply the proposed mathematical model in the analysis of archaeological finds.

Conclusions

The fundamental starting point for spectrometric analysis is the necessity of using certified reference materials suitable for archaeological research. The analysis of the Cultural Heritage Alloy Reference Materials (CHARM) set for copper alloys was carried out. Handheld (pXRF) and stationary energy dispersive (ED-XRF) spectrometers were used to investigate the elemental composition of the surfaces of the CHARM series standards and their drilled samples (shavings).

The analysis made it possible to conclude that the best agreement was found with the first, second and third CHARM. However, this observation is only valid for the pXRF measurements as the ED-XRF biases are larger. The pXRF measurements were the basis for the choice of further analysis of the mentioned CHARM due to higher precision and lower variation.

It has been established that the higher and lower trends in metal proportions in alloys might be identified by pXRF and ED-XRF spectrometers respectively. The results show that the percentage values of the pXRF and ED-XRF measurements differ quite significantly from the reported mean values of the standard. However, this quite significant bias is in line with the inherent capabilities of XRF spectrometry. The pXRF measurements are noticeably more accurate and less variable compared to the values obtained by ED-XRF spectrometer. The bias of the drilled shavings tests is significantly higher compared to the reference surface. This conclusion is valid for the results of the pXRF and ED-XRF drilled shavings test. However, the pXRF results are more accurate here too.

The XGBoost prediction model was created to convert the measurement values obtained by both spectrometers into reference values by minimising the differences between the values obtained and the values of the standards as given by the producer. As a result of the analysis of large-scale standards and drilled shavings, a mathematical model (XGBoost) has been selected which corrects the values of the composition of the standards and shavings based on the data obtained by the pXRF and ED-XRF to the known values of the standards, and thus minimises the bias. The analysis performed was to experimentally match the uneven surface of the CRM shavings and the configuration surface of the archaeological finds. The magnitude of the bias found between the smooth and the uneven surface of the shavings in the archaeological finds analysis might be interpreted and evaluated as an inaccuracy due to both the configuration of the find and partial corrosion.

Acknowledgements

This study was supported by the Research Council of Lithuania under grant award number S-MIP-19-50. We are grateful to the two anonymous reviewers for their remarks and comments, which gave us the possibility to improve the article text.

Abbreviations

Anal. Chim. Acta – Analytica Chimica Acta

Archaeol. Baltica – Archaeologica Baltica

Archaeol. Rec. – The SAA Archaeological Record

Herit. Sci. – Heritage Science

J. Anal. At. Spectrom. – Journal of Analytical Atomic Spectrometry

J. Archaeol. Sci. – Journal of Archaeological Science

Mater. Manuf. Process. – Materials and Manufacturing Processes

Microsc. Microanal. – Microscopy and Microanalysis

Spectrochim. Acta B At. Spectrosc. – Spectrochimica Acta Part B: Atomic Spectroscopy

Museum

LNM AR – Lithuanian National Museum, Department of archaeology, Vilnius

MLIM – Lithuanian Minor History Museum, Klaipėda

MM – Mažeikiai Museum, Mažeikiai

References

Almgren, O., 1897. *Studien* über *Nordeuropäische Fibelformen der ersten nachchristlichen Jahrhunderte, mit Berücksichtigung der provinzialrömischen und südrussischen Formen*. Stockholm.

Bayley, J. and Butcher, S., 2004. *Roman brooches in Britain: a technological and typological study based on the Richborough collection* (Reports of the Research Committee of the Society of Antiquaries of London, 68). London: The Society of Antiquaries of London.

Bezzenberger, A., 1904. *Analysen vorgeschichtlicher Bronzen Ostpreussens*. Königsberg i. Pr.: Gräfe & Unzer.

Bliujienė, A., Peseckas, K., Šapolaitė, J., Ežerinskis, Ž., Bagdzevičienė, J., Babenskas, E., Taraškevičius, R., Suzdalev, S., Vybernaitė-Lubienė, I., Pabedinskas, A., Butkus, L., Petrauskas, G., 2021a. Manufacture of the well-known Central and Northeastern European eye fibulae: previously unknown tricks of the trade. *Radiocarbon*, 63 (5), 1369–1386. https://doi.org/10.1017/RDC.2021.69

Bliujienė, A., Petrauskas, G., Bagdzevičienė, J., Babenskas, E., Rimkus, T., 2021b. Essential changes in the composition of copper alloys reveal technological diversities in the transition from the Earliest Iron Age to the Early Roman period in Lithuania. *Archaeol. Baltica*, 28, 39–62. https://doi.org/10.15181/ab.v28i0.2281

Bliujienė, A., Suzdalev, S., Vybernaitė-Lubienė, I., Bagdzevičienė, J., Petrauskas, G., Jatautis, Š., Babenskas, E., Senulis, S. and Šatavičė, E., 2023. *I–XIV amžių radinių iš vario lydinių archeometrinių duomenų bazė / Archaeometric database of copper alloy finds from the 1st to 14th centuries.* Open access database. Available from: http://lydiniai.lt/ [Accessed 4 September 2023].

Bos, M., Vrielink, J.A.M., van der Linden, W.E., 2000. Non-destructive analysis of small irregularly shaped homogeneous samples by X-ray fluorescence spectrometry. *Anal. Chim. Acta*, 412 (1–2), 203–211. https://doi.org/10.1016/S0003-2670(00)00771-6

Carter, G.F., Caley, E.R., Carlson, J.H., Carriveau, G.W., Hughes, M.J., Rengan, K., Segebade, C., 1983. Comparison of analyses of eight Roman orichalcum coin fragments by seven methods. *Archaeometry*, 25 (2), 201–213. https://doi.org/10.1111/j.1475-4754.1983.tb00677.x

Dungworth, D.B. 1997. Roman copper alloys: analysis of artefacts from northern Britain. *J. Archaeol. Sci*, 24, 901–910. http://dx.doi.org/10.1006/jasc.1996.0169

Fernandes, R., van Os. B.J.H. and Huisman, D.J., 2013. The use of hand-held XRF for investigating the composition and corrosion of Roman copper-alloyed artefacts. *Heritage Science*, September, 1 (30), 1–7. DOI:10.1186/2050-7445-1-30

Ferretti, M., 2014. The investigation of ancient metal artefacts by portable X-ray fluorescence devices. *J. Anal. At. Spectrom.*, 29, 1753–1766. https://doi.org/10.1039/C4JA00107A

Frahm, E., 2013a. Is obsidian sourcing about geochemistry or archaeology? A reply to Speakman and Shackley. *J. Archaeol. Sci.*, 40 (2), 1444–1448. http://dx.doi.org/10.1016/j.jas.2012.10.001

Frahm, E., 2013b. Validity of "off-the-shelf" handheld portable XRF for sourcing Near Eastern obsidian chip debris. *J. Archaeol. Sci.*, 40 (2), 1080–1092. https://doi.org/10.1016/j.jas.2012.06.038

Frahm, E., Doonan, R.C.P., 2013. The technological versus methodological revolution of portable XRF in archaeology. *J. Archaeol. Sci.*, 40 (2), 1425–1434. http://dx.doi.org/10.1016/j.jas.2012.10.013

Gigante, G.E, Ricciardi, P., Ridülfi, S., 2005. Areas and limits of employment of portable EDXRF equipment for *in situ* investigations. *ArchéoSciences*, 29, 51–59. https://doi.org/10.4000/archeosciences.488

Heginbotham, A., 2018. *The optimization and application of quantitative energy dispersive X-ray fluorescence spectroscopy to the collaborative study of historic copper alloys.* Thesis (PhD). Vrije Universiteit Amsterdam.

Heginbotham, A., Bassett, J., Bourgarit, D., Eveleigh, C., Glinsman, L., Hook, D., Smith, D., Speakman, R.J., Shugar, A., van Langh, R., 2015. The copper CHARM set: a new set of certified reference materials for the standardization of quantitative X-ray fluorescence analysis of heritage copper alloys. *Archaeometry,* 57 (5), 856–868. https://doi.org/10.1111/arcm.12117

Heginbotham, A., Bezur, A., Bouchard, M., Davis, J.M., Eremin, K., Frantz, J.H., Glinsman, L., Hayek, L.-A., Hook, D., Kantarelou, V., Karydas, A.G., Lee, L., Mass, J., Matsen, C., McCarthy, B., McGath, M., Shugar, A., Sirois, J., Smith, D. and Speakman, R.J., 2011. An evaluation of inter-laboratory repro-

ducibility for quantitative XRF of historic copper alloys. In: P. Mardikian, C. Chemello, C. Watters and P. Hull, eds. *Metal 2010: international conference on metal conservation. Interim meeting of the International Council of Museums Committee for Conservation Metal Working Group. October 11-15, 2010. Charleston, South Carolina, USA*. Clemson, SC: Clemson University, pp. 178–188.

Heginbotham, A., Solé, V.A., 2017. CHARMed PyMca, part I: a protocol for improved inter-laboratory reproducibility in the quantitative ED-XRF analysis of copper alloys. *Archaeometry*, 59 (4), 714–730. https://doi.org/10.1111/arcm.12282

Hoffmann, P., 2006. Non-invasive identification of chemical compounds by EDXRS. In: B. Beckhoff, B. *Kanngießer, N. Langhoff, R. Wedell* and H. *Wolff, eds. Handbook of practical X-ray fluorescence analysis*. Heidelberg: Springer Berlin, pp. 769–783.

Injuk, J., van Grieken, R., Blank, A., Eksperiandova, L. and Buhrke, V., 2006. Specimen preparation. In: B. Beckhoff, B. *Kanngießer, N. Langhoff, R. Wedell* and H. *Wolff, eds. Handbook of practical X-ray fluorescence analysis*. Heidelberg: Springer Berlin, pp. 411–432. https://doi.org/10.1007/978-3-540-36722-2_6

Jouttijärvi, A., 2017. Roman alloying practice. *Mater. Manuf. Process.*, 32 (7–8), 813–826. https://doi.org/10.1080/10426914.2017.1279325

Lam, T., 2021. Comparison of quantification from field deployable pXRF and laboratory based-micro-XRF within an SEM of Cu-based alloys. *Microsc. Microanal.*, 27 (S1), 3200–3202. https://doi.org/10.1017/S1431927621011053

Liritzis, I. and Zacharias, N., 2011. Portable XRF of archaeological artifacts: current research, potentials and limitations. In: M. Shackley, ed. *X-ray fluorescence spectrometry (XRF) in geoarchaeology.* New York, NY: Springer, pp. 109–142. https://doi.org/10.1007/978-1-4419-6886-9_6

Lutz, J. Pernicka, E., 1996. Energy dispersive X-ray fluorescence analysis of ancient copper alloys: empirical values for precision and accuracy. *Archaeometry*, 38 (2), 313–323. https://doi.org/10.1111/j.1475-4754.1996.tb00779.x

Mantler, M., Willis, J., Lachance, G., Vrebos, B.A.R., Mauser, K.-E., Kawahara, N., Rousseau, R.M. and Brouwer, P.N., 2006. Quantitative analysis. In: B. Beckhoff, B. *Kanngießer, N. Langhoff, R. Wedell* and H. *Wolff, eds. Handbook of practical X-ray fluorescence analysis*. Heidelberg: Springer Berlin, pp. 309–410. Heidelberg: Springer Berlin. https://doi.org/10.1007/978-3-540-36722-2_5

Northover, J.P., Rychner, V., 1998. Bronze analysis: experience of a comparative programme. In: C. Mordant, M. Pernot and V. Rychner, eds. *L'atelier du bronzier en Europe du XX^e au VIII^e siècle avant notre ère. Actes du Colloque International* "*Bronze '96*", de Neuchâtel et Dijon 1996. 1. Les analyses de composition du métal: leur apport à l'archéologie du l'Âge du Bronze. Paris: Èditions du CTHS, pp. 19–40.

Oudbashi, O., Emami, S.M., Ahmadi, H., Davami, P., 2013. Micro-stratigraphical investigation on corrosion layers in ancient Bronze artefacts by scanning electron microscopy energy dispersive spectrometry and optical microscopy. *Herit. Sci.*, 1 (21), 1–10. https://doi.org/10.1186/2050-7445-1-21

Pollard, A.M., Bray, P., Cuénod, A., Hommel, P., Hsu, Y-K., Liu, R., Perucchetti, L., Pouncett, J. and Saunders, M., 2018. *Beyond provenance: new approaches to interpreting the chemistry of archaeological copper alloys* (Studies in Archaeological Sciences, 6). Leuven: Leuven University Press.

Pollard, A.M., Bray, P., Gosden, C., Wilson, A., Hamerow, H., 2015. Characterising copper-based metals in Britain in the first millennium AD: a preliminary quantification of metal flow and recycling. *Antiquity*, 89 (345), 697–713. https://doi.org/10.15184/aqy.2015.20

Porcinai, S., Cagnini, A., Galeotti, M., Ferretti, M., 2023. Quantitative analysis of copper alloys by means of portable X-ray fluorescence: A comparison between analysis of shavings and surfaces. *Spectrochimica Acta Part B: Atomic Spectroscopy,* Available online 14 October 2023, https://doi.org/10.1016/j.sab.2023.106808.

Rehren Th. 1999. The same … … but different: A juxtaposition of Roman and Medieval brass making in Central Europe. In: S.M.M. Young, M. Pollard, P. Budd, and R. Ixer, eds. *Metals in Antiquity* (= BAR International Series 792). Oxford: Archaeopress, pp. 252–257.

Roxburgh, M.A., 2019. *From the fabricae of Augustus and the workshops of Charlemagne: a compositional study of corroded copper-alloy artifacts using hand-held portable XRF.* Thesis (PhD). Leiden University.

Roxburgh, M.A., Heeren, S., Huisman, D.J., van Os, B.J.H., 2019. Non-destructive survey of early Roman copper-alloy brooches using portable X-ray fluorescence spectrometry. *Archaeometry*, 61 (1), 55–69. https://doi.org/10.1111/arcm.12414

Roxburgh, M.A., Olli, M., 2018. Eyes to the North: a multi-element analysis of copper-alloy eye brooches in the eastern Baltic, produced during the Roman Iron Age. *Germania*, 96, 209–233. https://doi.org/10.11588/ger.2018.66174

Shackley, M.S., 2010. Is there reliability and validity in portable X-ray fluorescence spectrometry (PXRF)? *Archaeol. Rec.*, 10 (5), 17–20.

Shackley, M.S., 2011. An introduction to X-ray fluorescence (XRF) analysis in archaeology. In: M. Shackley, ed. *X-ray fluorescence spectrometry (XRF) in geoarchaeology.* New York, NY: Springer, pp. 7–44. https://doi.org/10.1007/978-1-4419-6886-92

Shugar, A.N., 2013. Portable X-ray fluorescence and archaeology: limitations of the instrument and suggested methods to achieve desired results. In: R.A. Armitage and J.H. Burton, eds. *Archaeological Chemistry*, VIII (ACS Symposium Series, 1147). Washington, DC: American Chemical Society, pp. 173–193. https://doi.org/10.1021/bk-2013-1147.ch010

Sitko, R., Zawisza, B., 2005. Calibration of wavelength-dispersive X-ray spectrometer for standardless analysis. *Spectrochim. Acta B At. Spectrosc.,* 60 (1), 95–100. https://doi.org/10.1016/j.sab.2004.11.004

Speakman, R.J., Shackley, M.S., 2013. Silo science and portable XRF in archaeology: a response to Frahm. *J. Archaeol. Sci.*, 40 (2), 1435–1443. https://doi.org/10.1016/j.jas.2012.09.033

Steenstra, E.S., Berndt, J., Klemme, S., van Westrenen, W., Heginbotham, A., Davies, G.R., 2022. Analysis of the CHARM Cu-alloy reference materials using excimer ns-LA-ICP-MS: assessment of matrix effects and applicability to artefact provenancing. *Archaeometry*, 64 (3), 655–670. https://doi.org/10.1111/arcm.12729

Vaitkunskienė, L., Merkevičius, A., 1978. Spalvotųjų metalų dirbiniai ir jų gamyba. *Lietuvių materialinė kultūra IX–XIII amžiuje*, I, 89–116.

Van der Meulen van der Veen, B.S. 2023. Chemical compositional data of the corrosion products on Late Roman military crossbow brooches. A comparative study. *J. Archaeol. Sci.: Reports,* 43. https://doi.org/10.1016/j.jasrep.2023.103839

Kultūros paveldo etalonų patikimumo vertinimas rentgeno fluorescencijos metodu, naudojant rankinės ir energijos dispersijos rentgeno spindulių fluorescencijos paviršių matavimo spektrometrus

Audronė Bliujienė, Šarūnas Jatautis, Sergej Suzdalev, Gediminas Petrauskas

Santrauka

Šiame straipsnyje aptariami penkių kultūros paveldo lydinių etaloninių medžiagų (CHARM) ir jų drožlių didelės apimties tyrimai (1, 2 lentelė, 1 priedas). Jie atlikti naudojant rankinį rentgeno spindulių fluorescencijos (pXRF) bei stacionarų energijos dispersijos ir rentgeno spindulių fluorescencijos (ED-XRF) spektrometrus. Pagrindinis šių tyrimų tikslas – įvertinti pXRF ir ED-XRF fluorescencinės spektrometrijos ir pačių spektrometrų galimybes (2 pav.). Rentgeno spindulių fluorescencija yra neardantis radinio paviršiaus matavimo metodas. Siekta įvertini kultūros paveldo pamatinių medžiagų tyrimais gautų duomenų patikimumą. Antrasis tikslas – įvertinti galimybes pXRF ir ED-XRF spektrometrų, naudotų analizuojant tų pačių penkių etaloninių medžiagų drožles (1 pav.). Norint pasiekti šiuos tikslus, reikėjo rasti tinkamiausias analitines priemones duomenims palyginti, įvertinti ir patikimumui užtikrinti, ir svarbiausia – sukurti patikimus duomenų analizės ir rezultatų patvirtinimo patikros modelius (3–5 pav., 3 lentelė).

Remiantis kultūros paveldo lydinių etaloninių medžiagų analize, galima daryti išvadą, kad rankinės rentgeno spindulių fluorescencijos spektrometrijos rezultatai, gauti abiem spektrometrais, yra patikimi ir gali būti lyginami tarpusavyje, atsižvelgiant į keturias pagrindines sąlygas: analizė gali būti grįsta sertifikuotomis etaloninėmis medžiagomis su žinoma jų elementine sudėtimi; gali būti atliekama pagal tinkamą matavimo metodiką (tyrimo protokolą); gali būti aiškiai apibrėžtos analizės priemonės (prognostinė analizė); galiausiai gali būti atliekami tyrimai su archeologiniais artefaktais (6 pav.). Siekiant nustatyti galimybę sėkmingai taikyti XRF spektrometriją tiriant archeologinius artefaktus, pagamintus iš vario lydinių, buvo įvertintas gautų rezultatų patikimumas ir tarpusavio koreliacija.

Appendix

Appendix 1. Various descriptive statistics for CHARM standards and drilled samples (shavings) Prepared by Jatautis.

Reference	Method	Type	Metal	Mean	Median	95% CI Lower	95% CI Upper	95% CI Length	First quartile	Third quartile	IQR	Standard deviation	Reference value	Mean absolute difference	Median absolute difference	Mean absolute percentage difference	Median absolute percentage difference
1-CHARM (32X SN6.B)	pXRF	Solid	Ag	0.98	0.95	0.96	1.01	0.05	0.94	0.96	0.03	0.2	1.01	0.1	0.06	9.06	5.94
1-CHARM (32X SN6.B)	pXRF	Solid	As	0	0	0	0	0	0	0	0	0	0.8	0.8	0.8		
1-CHARM (32X SN6.B)	pXRF	Solid	Bi	0.16	0.13	0.14	0.18	0.04	0.11	0.14	0.02	0.17	0.13	0.05	0.01	13.02	8.55
1-CHARM (32X SN6.B)	pXRF	Solid	Co	0.76	0.79	0.74	0.77	0.03	0.76	0.8	0.04	0.14	0.75	0.07	0.04	26.04	5.49
1-CHARM (32X SN6.B)	pXRF	Solid	Cu	86.17	86.5	85.94	86.41	0.47	86.33	86.65	0.32	2	85.73	1.19	0.79	1.42	0.91
1-CHARM (32X SN6.B)	pXRF	Solid	Fe	0.38	0.39	0.38	0.39	0.01	0.35	0.42	0.07	0.05	0.38	0.04	0.03	11.51	8.36
1-CHARM (32X SN6.B)	pXRF	Solid	Mn	0.09	0.09	0.08	0.09	0	0.09	0.1	0.01	0.02	0.09	0.01	0		5.26
1-CHARM (32X SN6.B)	pXRF	Solid	Ni	0.31	0.32	0.31	0.32	0.01	0.32	0.33	0.02	0.04	0.3	0.04	0.03	14.04	9.79
1-CHARM (32X SN6.B)	pXRF	Solid	Pb	1.58	1.57	1.57	1.59	0.02	1.55	1.61	0.06	0.1	1.64	0.09	0.08	6.05	5.05
1-CHARM (32X SN6.B)	pXRF	Solid	Sb	0.3	0.29	0.3	0.3	0.01	0.29	0.3	0.02	0.03	0.3	0.02	0.01	5.79	4.11
1-CHARM (32X SN6.B)	pXRF	Solid	Sn	6.59	6.86	6.47	6.72	0.25	6.79	6.97	0.18	1.07	6.78	0.46	0.16	15.49	2.35
1-CHARM (32X SN6.B)	pXRF	Solid	Zn	2.56	1.98	2.24	2.89	0.65	1.96	2.01	0.05	2.79	2	0.62	0.03	5.36	1.3
1-CHARM (32X SN6.B)	ED-XRF	Solid	Ag	1.82	1.84	1.76	1.89	0.14	1.83	1.85	0.02	0.25	1.01	0.85	0.83	144.8	45.21
1-CHARM (32X SN6.B)	ED-XRF	Solid	As	0.55	0.56	0.53	0.57	0.04	0.54	0.58	0.04	0.08	0.8	0.25	0.24	73132.12	43.16

Appendix. Continuation

Reference	Method	Type	Metal	Mean	Median	95% CI Lower	95% CI Upper	95% CI Length	First quartile	Third quartile	IQR	Standard deviation	Reference value	Mean absolute difference	Median absolute difference	Mean absolute percentage difference	Median absolute percentage difference
1-CHARM (32X SN6.B)	ED-XRF	Solid	Bi	0.03	0.03	0.03	0.04	0.01	0.02	0.05	0.03	0.02	0.13	0.09	0.09	15799.57	288.38
1-CHARM (32X SN6.B)	ED-XRF	Solid	Co	0.73	0.75	0.7	0.75	0.05	0.72	0.75	0.03	0.09	0.75	0.02	0.01	25.43	0.96
1-CHARM (32X SN6.B)	ED-XRF	Solid	Cu	78.21	78.49	77.89	78.53	0.64	78.43	78.55	0.12	1.18	85.73	7.52	7.24	9.65	9.22
1-CHARM (32X SN6.B)	ED-XRF	Solid	Fe	0.43	0.4	0.37	0.49	0.12	0.39	0.4	0.01	0.22	0.38	0.05	0.03	6.85	6.33
1-CHARM (32X SN6.B)	ED-XRF	Solid	Mn	0.12	0.09	0.06	0.17	0.11	0.08	0.1	0.01	0.2	0.09	0.03	0.01	7.53	6.03
1-CHARM (32X SN6.B)	ED-XRF	Solid	Ni	0.34	0.26	0.22	0.46	0.25	0.25	0.34	0.09	0.45	0.3	0.1	0.05	17.5	15.19
1-CHARM (32X SN6.B)	ED-XRF	Solid	Pb	0.76	0.78	0.73	0.79	0.06	0.73	0.8	0.07	0.11	1.64	0.88	0.87	183.96	111.94
1-CHARM (32X SN6.B)	ED-XRF	Solid	Sb	0.61	0.6	0.58	0.63	0.05	0.59	0.61	0.01	0.09	0.3	0.32	0.3	179.62	49.26
1-CHARM (32X SN6.B)	ED-XRF	Solid	Sn	14.07	13.9	13.5	14.64	1.13	13.81	13.98	0.17	2.1	6.78	7.53	7.12	182.59	51.22
1-CHARM (32X SN6.B)	ED-XRF	Solid	Zn	1.68	1.7	1.64	1.71	0.07	1.67	1.71	0.04	0.13	2	0.32	0.3	20.92	17.51
2-CHARM (31X 78359.B)	pXRF	Solid	Ag	1.88	1.92	1.86	1.9	0.04	1.87	1.94	0.07	0.17	2.01	0.14	0.09	13.31	4.95
2-CHARM (31X 78359.B)	pXRF	Solid	As	0	0	0	0	0	0	0	0	0	0.1	0.1	0.1		
2-CHARM (31X 78359.B)	pXRF	Solid	Bi	0.89	0.92	0.88	0.9	0.02	0.82	0.96	0.14	0.09	0.91	0.07	0.07	9.45	7.52

Reference	Method	Type	Metal	Mean	Median	95% CI Lower	95% CI Upper	95% CI Length	First quartile	Third quartile	IQR	Standard deviation	Reference value	Mean absolute difference	Median absolute difference	Mean absolute percentage difference	Median absolute percentage difference
2-CHARM (31X 78359.B)	pXRF	Solid	Co	0.12	0.12	0.12	0.12	0	0.12	0.12	0.01	0.01	0.11	0.01	0.01	10.58	7.38
2-CHARM (31X 78359.B)	pXRF	Solid	Cu	77.26	77.38	77.09	77.44	0.34	77.12	77.5	0.37	1.42	76.6	0.89	0.78	1.19	1.01
2-CHARM (31X 78359.B)	pXRF	Solid	Fe	0.19	0.19	0.19	0.19	0.01	0.17	0.21	0.03	0.02	0.19	0.02	0.02	10.71	7.91
2-CHARM (31X 78359.B)	pXRF	Solid	Mn	0	0	0	0.01	0.01	0	0	0	0.02	0	0.01	0		
2-CHARM (31X 78359.B)	pXRF	Solid	Ni	0.2	0.2	0.19	0.2	0.01	0.2	0.21	0.01	0.03	0.2	0.02	0.01	10.91	3.92
2-CHARM (31X 78359.B)	pXRF	Solid	Pb	1.05	1.04	1.05	1.06	0.02	1.02	1.08	0.05	0.07	1.04	0.04	0.03	4	2.45
2-CHARM (31X 78359.B)	pXRF	Solid	Sb	0.42	0.42	0.42	0.42	0.01	0.41	0.44	0.03	0.03	0.44	0.02	0.02	6.29	4.56
2-CHARM (31X 78359.B)	pXRF	Solid	Sn	1.52	1.56	1.51	1.54	0.04	1.54	1.57	0.04	0.15	1.6	0.09	0.05	13.71	2.96
2-CHARM (31X 78359.B)	pXRF	Solid	Zn	16.06	15.88	15.85	16.28	0.43	15.79	15.99	0.21	1.76	16.26	0.54	0.39	2.85	2.43
2-CHARM (31X 78359.B)	ED-XRF	Solid	Ag	4.25	4.24	4.23	4.27	0.04	4.21	4.26	0.05	0.08	2.01	2.24	2.22	52.62	52.47

Appendix. Continuation

Reference	Method	Type	Metal	Mean	Median	95% CI Lower	95% CI Upper	95% CI Length	First quartile	Third quartile	IQR	Standard deviation	Reference value	Mean absolute difference	Median absolute difference	Mean absolute percentage difference	Median absolute percentage difference
2-CHARM (31X 78359.B)	ED-XRF	Solid	As	0.06	0.06	0.06	0.06	0	0.05	0.07	0.01	0.01	0.1	0.04	0.04	66.96	65.85
2-CHARM (31X 78359.B)	ED-XRF	Solid	Bi	0.64	0.64	0.64	0.64	0.01	0.63	0.65	0.03	0.02	0.91	0.27	0.27	42.44	42.61
2-CHARM (31X 78359.B)	ED-XRF	Solid	Co	0.1	0.11	0.1	0.11	0	0.1	0.11	0.01	0.01	0.11	0.01	0	8.71	3.67
2-CHARM (31X 78359.B)	ED-XRF	Solid	Cu	74.21	74.23	74.16	74.25	0.09	74.2	74.28	0.08	0.2	76.6	2.39	2.37	3.22	3.19
2-CHARM (31X 78359.B)	ED-XRF	Solid	Fe	0.2	0.2	0.2	0.2	0	0.2	0.21	0	0.01	0.19	0.01	0.01	5.23	5.86
2-CHARM (31X 78359.B)	ED-XRF	Solid	Mn	0.01	0.01	0.01	0.01	0	0.01	0.01	0	0	0	0	0	311.69	39.27
2-CHARM (31X 78359.B)	ED-XRF	Solid	Ni	0.17	0.16	0.17	0.18	0.01	0.15	0.18	0.02	0.03	0.2	0.04	0.04	21.71	20.69
2-CHARM (31X 78359.B)	ED-XRF	Solid	Pb	0.63	0.65	0.63	0.64	0.02	0.62	0.66	0.04	0.04	1.04	0.41	0.4	65.27	61.27
2-CHARM (31X 78359.B)	ED-XRF	Solid	Sb	0.99	0.98	0.98	1	0.02	0.97	1	0.03	0.05	0.44	0.55	0.54	55.68	55.14
2-CHARM (31X 78359.B)	ED-XRF	Solid	Sn	3.43	3.38	3.4	3.47	0.07	3.34	3.42	0.07	0.16	1.6	1.83	1.78	53.3	52.66

Reference	Method	Type	Metal	Mean	Median	95% CI Lower	95% CI Upper	95% CI Length	First quartile	Third quartile	IQR	Standard deviation	Reference value	Mean absolute difference	Median absolute difference	Mean absolute percentage difference	Median absolute percentage difference
2-CHARM (31X 78359.B)	ED-XRF	Solid	Zn	14.52	14.53	14.51	14.53	0.02	14.51	14.55	0.04	0.04	16.26	1.74	1.73	11.97	11.91
3-CHARM (31X TB5.B)	pXRF	Solid	Ag	0.16	0.2	0.14	0.17	0.03	0	0.21	0.21	0.14	0.22	0.07	0.01		7.46
3-CHARM (31X TB5.B)	pXRF	Solid	As	0	0	0	0	0	0	0	0	0	0.4	0.4	0.4		
3-CHARM (31X TB5.B)	pXRF	Solid	Bi	0.29	0.29	0.28	0.3	0.01	0.26	0.31	0.05	0.06	0.29	0.03	0.03		8.96
3-CHARM (31X TB5.B)	pXRF	Solid	Co	0.02	0.02	0.02	0.02	0	0.02	0.02	0.01	0.01	0.02	0	0		15.83
3-CHARM (31X TB5.B)	pXRF	Solid	Cu	61.74	61.6	61.59	61.89	0.31	61.38	61.76	0.38	1.33	61.49	0.5	0.22	0.78	0.36
3-CHARM (31X TB5.B)	pXRF	Solid	Fe	0.1	0.09	0.09	0.11	0.02	0.08	0.1	0.02	0.1	0.09	0.02	0.01	15.77	13.25
3-CHARM (31X TB5.B)	pXRF	Solid	Mn	0.3	0.29	0.28	0.33	0.04	0.28	0.29	0.01	0.19	0.28	0.03	0.01		2.41
3-CHARM (31X TB5.B)	pXRF	Solid	Ni	0.11	0.11	0.11	0.12	0.01	0.11	0.12	0.01	0.03	0.11	0.01	0.01	11.84	6.19
3-CHARM (31X TB5.B)	pXRF	Solid	Pb	0.61	0.58	0.58	0.63	0.05	0.56	0.6	0.04	0.2	0.57	0.05	0.02	5.35	3.36
3-CHARM (31X TB5.B)	pXRF	Solid	Sb	0.23	0.23	0.22	0.23	0.01	0.22	0.24	0.01	0.04	0.23	0.01	0.01	8.57	2.97
3-CHARM (31X TB5.B)	pXRF	Solid	Sn	0.15	0.13	0.13	0.17	0.04	0.12	0.14	0.02	0.18	0.13	0.03	0.01	10	6.61
3-CHARM (31X TB5.B)	pXRF	Solid	Zn	35.79	35.97	35.58	36.01	0.43	35.85	36.13	0.28	1.85	35.62	0.71	0.37	2.41	1.03
3-CHARM (31X TB5.B)	ED-XRF	Solid	Ag	0.53	0.47	0.42	0.65	0.24	0.47	0.48	0.01	0.47	0.22	0.32	0.26	55.13	54.44
3-CHARM (31X TB5.B)	ED-XRF	Solid	As	0.33	0.34	0.32	0.34	0.02	0.33	0.34	0.01	0.04	0.4	0.06	0.06	25.93	17.02
3-CHARM (31X TB5.B)	ED-XRF	Solid	Bi	0.21	0.2	0.2	0.23	0.03	0.19	0.22	0.02	0.05	0.29	0.09	0.09	43.48	43.91

Appendix. Continuation

Reference	Method	Type	Metal	Mean	Median	95% CI Lower	95% CI Upper	95% CI Length	First quartile	Third quartile	IQR	Standard deviation	Reference value	Mean absolute difference	Median absolute difference	Mean absolute percentage difference	Median absolute percentage difference
3-CHARM (31X TB5.B)	ED-XRF	Solid	Co	0.01	0.01	0.01	0.02	0.01	0	0.02	0.01	0.01	0.02	0.01	0.01	2677.92	60.83
3-CHARM (31X TB5.B)	ED-XRF	Solid	Cu	61.52	61.29	61.11	61.93	0.82	61.27	61.38	0.11	1.63	61.49	0.38	0.21	0.56	0.34
3-CHARM (31X TB5.B)	ED-XRF	Solid	Fe	0.1	0.1	0.1	0.1	0.01	0.1	0.1	0.01	0.01	0.09	0.01	0.01	7.26	6.56
3-CHARM (31X TB5.B)	ED-XRF	Solid	Mn	0.29	0.3	0.28	0.3	0.02	0.28	0.31	0.03	0.04	0.28	0.02	0.02	53.27	7.18
3-CHARM (31X TB5.B)	ED-XRF	Solid	Ni	0.1	0.09	0.1	0.11	0.01	0.09	0.12	0.03	0.02	0.11	0.02	0.02	18.62	18.59
3-CHARM (31X TB5.B)	ED-XRF	Solid	Pb	0.4	0.4	0.38	0.41	0.02	0.36	0.42	0.06	0.04	0.57	0.18	0.17	47.15	43.36
3-CHARM (31X TB5.B)	ED-XRF	Solid	Sb	0.55	0.54	0.53	0.56	0.03	0.53	0.54	0.01	0.06	0.23	0.32	0.31	57.87	57.44
3-CHARM (31X TB5.B)	ED-XRF	Solid	Sn	0.35	0.3	0.26	0.45	0.19	0.3	0.31	0.01	0.39	0.13	0.23	0.17	58.37	57.55
3-CHARM (31X TB5.B)	ED-XRF	Solid	Zn	33.83	34.15	33.2	34.45	1.25	34.08	34.18	0.1	2.47	35.62	1.79	1.47	6.58	4.3
8-CHARM (33X GM21.B)	pXRF	Solid	Ag	0.67	0.68	0.67	0.68	0.01	0.66	0.69	0.03	0.03	0.7	0.03	0.02	4.74	2.77
8-CHARM (33X GM21.B)	pXRF	Solid	As	0	0	0	0	0	0	0	0	0	0.33	0.33	0.33		
8-CHARM (33X GM21.B)	pXRF	Solid	Bi	0.35	0.36	0.35	0.36	0.01	0.32	0.38	0.06	0.03	0.46	0.11	0.1	30.87	28.93
8-CHARM (33X GM21.B)	pXRF	Solid	Co	0.13	0.13	0.13	0.13	0	0.13	0.14	0.01	0.01	0	0.13	0.13	100	100
8-CHARM (33X GM21.B)	pXRF	Solid	Cu	81.39	81.43	81.34	81.45	0.11	81.15	81.54	0.4	0.37	78.86	2.53	2.57	3.11	3.15

Reference	Method	Type	Metal	Mean	Median	95% CI Lower	95% CI Upper	95% CI Length	First quartile	Third quartile	IQR	Standard deviation	Reference value	Mean absolute difference	Median absolute difference	Mean absolute percentage difference	Median absolute percentage difference
8-CHARM (33X GM21.B)	pXRF	Solid	Fe	0.71	0.72	0.7	0.72	0.02	0.7	0.75	0.05	0.06	0.69	0.05	0.04	7.32	5.97
8-CHARM (33X GM21.B)	pXRF	Solid	Mn	0.04	0.05	0.04	0.05	0	0.04	0.05	0.01	0.01	0	0.04	0.05	100	100
8-CHARM (33X GM21.B)	pXRF	Solid	Ni	0.2	0.2	0.2	0.2	0.01	0.19	0.21	0.01	0.02	0.2	0.01	0.01	7.42	3.9
8-CHARM (33X GM21.B)	pXRF	Solid	Pb	5.73	5.7	5.71	5.76	0.05	5.62	5.83	0.21	0.18	7.53	1.8	1.83	31.44	32.04
8-CHARM (33X GM21.B)	pXRF	Solid	Sb	1.02	1.02	1.01	1.02	0.01	1	1.04	0.05	0.04	1.03	0.03	0.02	3.3	2.38
8-CHARM (33X GM21.B)	pXRF	Solid	Sn	4.42	4.45	4.38	4.45	0.07	4.39	4.54	0.15	0.24	4.5	0.17	0.09	4.06	2.16
8-CHARM (33X GM21.B)	pXRF	Solid	Zn	4.87	4.86	4.86	4.88	0.02	4.81	4.91	0.1	0.08	4.96	0.11	0.1	2.2	2.07
8-CHARM (33X GM21.B)	ED-XRF	Solid	Ag	1.37	1.37	1.36	1.37	0	1.36	1.37	0.01	0.01	0.7	0.67	0.67	48.72	48.76
8-CHARM (33X GM21.B)	ED-XRF	Solid	As	0.25	0.25	0.25	0.26	0.01	0.24	0.27	0.02	0.01	0.33	0.08	0.08	31.07	30.74
8-CHARM (33X GM21.B)	ED-XRF	Solid	Bi	0.19	0.2	0.19	0.2	0.01	0.18	0.21	0.03	0.02	0.46	0.27	0.26	139.64	135.02
8-CHARM (33X GM21.B)	ED-XRF	Solid	Co	0.11	0.11	0.1	0.11	0.01	0.1	0.11	0.02	0.01	0	0.11	0.11	100	100

Appendix. Continuation

Reference	Method	Type	Metal	Mean	Median	95% CI Lower	95% CI Upper	95% CI Length	First quartile	Third quartile	IQR	Standard deviation	Reference value	Mean absolute difference	Median absolute difference	Mean absolute percentage difference	Median absolute percentage difference
8-CHARM (33X GM21.B)	ED-XRF	Solid	Cu	77.29	77.27	77.27	77.31	0.05	77.23	77.37	0.14	0.08	78.86	1.57	1.59	2.03	2.06
8-CHARM (33X GM21.B)	ED-XRF	Solid	Fe	0.71	0.71	0.71	0.71	0	0.7	0.72	0.01	0.01	0.69	0.02	0.02	2.72	3.05
8-CHARM (33X GM21.B)	ED-XRF	Solid	Mn	0.05	0.05	0.05	0.05	0	0.05	0.05	0	0	0	0.05	0.05	100	100
8-CHARM (33X GM21.B)	ED-XRF	Solid	Ni	0.19	0.17	0.18	0.2	0.02	0.16	0.24	0.08	0.04	0.2	0.04	0.04	19.88	19.89
8-CHARM (33X GM21.B)	ED-XRF	Solid	Pb	2.97	2.98	2.93	3	0.07	2.84	3.01	0.18	0.12	7.53	4.56	4.56	154.26	153.11
8-CHARM (33X GM21.B)	ED-XRF	Solid	Sb	2.21	2.2	2.2	2.21	0.01	2.19	2.22	0.03	0.01	1.03	1.17	1.17	53.19	53.13
8-CHARM (33X GM21.B)	ED-XRF	Solid	Sn	9.25	9.24	9.24	9.27	0.03	9.21	9.3	0.1	0.05	4.5	4.75	4.74	51.37	51.28
8-CHARM (33X GM21.B)	ED-XRF	Solid	Zn	4.41	4.41	4.41	4.42	0.01	4.41	4.42	0.01	0.01	4.96	0.55	0.55	12.36	12.37
9-CHARM (32X LB10.G)	pXRF	Solid	Ag	0	0	0	0	0	0	0	0	0	0.07	0.07	0.07		
9-CHARM (32X LB10.G)	pXRF	Solid	As	0	0	0	0	0	0	0	0	0	0.17	0.17	0.17		
9-CHARM (32X LB10.G)	pXRF	Solid	Bi	0.07	0.08	0.07	0.08	0.01	0.06	0.09	0.02	0.03	0.09	0.03	0.02		24

Reference	Method	Type	Metal	Mean	Median	95% CI Lower	95% CI Upper	95% CI Length	First quartile	Third quartile	IQR	Standard deviation	Reference value	Mean absolute difference	Median absolute difference	Mean absolute percentage difference	Median absolute percentage difference
9-CHARM (32X LB10.G)	pXRF	Solid	Co	0.1	0.1	0.1	0.1	0	0.09	0.11	0.01	0.01	0.08	0.02	0.02	15.21	16.42
9-CHARM (32X LB10.G)	pXRF	Solid	Cu	78.47	78.43	78.39	78.54	0.15	78.15	78.64	0.48	0.51	77.1	1.37	1.33	1.74	1.69
9-CHARM (32X LB10.G)	pXRF	Solid	Fe	0.01	0	0	0.01	0	0	0	0	0.02	0	0.01	0		
9-CHARM (32X LB10.G)	pXRF	Solid	Mn	0	0	0	0	0	0	0	0	0	0	0	0	100	100
9-CHARM (32X LB10.G)	pXRF	Solid	Ni	0.7	0.71	0.68	0.71	0.02	0.7	0.72	0.03	0.07	0.69	0.04	0.02	7.06	3.23
9-CHARM (32X LB10.G)	pXRF	Solid	Pb	11.85	11.83	11.82	11.88	0.07	11.65	12.02	0.36	0.23	12.6	0.75	0.77	6.38	6.5
9-CHARM (32X LB10.G)	pXRF	Solid	Sb	0.57	0.57	0.57	0.58	0.01	0.56	0.59	0.03	0.02	0.6	0.03	0.02	4.86	4.17
9-CHARM (32X LB10.G)	pXRF	Solid	Sn	8.06	8.15	7.99	8.12	0.13	8.04	8.27	0.23	0.44	8.29	0.33	0.18	4.34	2.19
9-CHARM (32X LB10.G)	pXRF	Solid	Zn	0.06	0.06	0.05	0.07	0.02	0	0.09	0.09	0.05	0.11	0.06	0.05		74.6
9-CHARM (32X LB10.G)	ED-XRF	Solid	Ag	0.11	0.11	0.11	0.11	0	0.11	0.11	0	0	0.07	0.04	0.04	38.33	38.31
9-CHARM (32X LB10.G)	ED-XRF	Solid	As	0.08	0.09	0.08	0.09	0.01	0.07	0.1	0.02	0.01	0.17	0.08	0.08	103.31	98.36

Appendix. Continuation

Reference	Method	Type	Metal	Mean	Median	95% CI Lower	95% CI Upper	95% CI Length	First quartile	Third quartile	IQR	Standard deviation	Reference value	Mean absolute difference	Median absolute difference	Mean absolute percentage difference	Median absolute percentage difference
9-CHARM (32X LB10.G)	ED-XRF	Solid	Bi	0.03	0.03	0.02	0.03	0.01	0.01	0.04	0.03	0.01	0.09	0.07	0.06	15534.74	211.04
9-CHARM (32X LB10.G)	ED-XRF	Solid	Co	0.08	0.08	0.07	0.08	0.01	0.06	0.08	0.02	0.01	0.08	0.01	0.01	17.43	8.1
9-CHARM (32X LB10.G)	ED-XRF	Solid	Cu	74.15	74.15	74.13	74.16	0.04	74.12	74.17	0.05	0.06	77.1	2.95	2.95	3.98	3.98
9-CHARM (32X LB10.G)	ED-XRF	Solid	Fe	0.01	0.01	0.01	0.01	0	0	0.01	0.01	0.01	0	0.01	0.01	222.32	91.91
9-CHARM (32X LB10.G)	ED-XRF	Solid	Mn	0	0	0	0	0	0	0	0	0	0	0	0	100	100
9-CHARM (32X LB10.G)	ED-XRF	Solid	Ni	0.66	0.63	0.64	0.67	0.03	0.62	0.71	0.09	0.04	0.69	0.05	0.06	7.51	8.97
9-CHARM (32X LB10.G)	ED-XRF	Solid	Pb	6.57	6.57	6.55	6.59	0.04	6.52	6.62	0.1	0.06	12.6	6.03	6.03	91.69	91.66
9-CHARM (32X LB10.G)	ED-XRF	Solid	Sb	1.2	1.2	1.19	1.2	0	1.19	1.2	0.01	0.01	0.6	0.6	0.6	49.93	49.96
9-CHARM (32X LB10.G)	ED-XRF	Solid	Sn	16.86	16.86	16.84	16.88	0.04	16.81	16.91	0.1	0.07	8.29	8.57	8.57	50.83	50.83
9-CHARM (32X LB10.G)	ED-XRF	Solid	Zn	0.09	0.09	0.08	0.09	0	0.08	0.09	0.01	0.01	0.11	0.02	0.02	27.55	28.81

Reference	Method	Type	Metal	Mean	Median	95% CI Lower	95% CI Upper	95% CI Length	First quartile	Third quartile	IQR	Standard deviation	Reference value	Mean absolute difference	Median absolute difference	Mean absolute percentage difference	Median absolute percentage difference
1-CHARM (32X SN6.B)	pXRF	Shavings	Ag	0.84	0.82	0.81	0.87	0.06	0.8	0.85	0.04	0.06	1.01	0.17	0.19	20.44	23.56
1-CHARM (32X SN6.B)	pXRF	Shavings	As	0	0	0	0	0	0	0	0	0	0.8	0.8	0.8		
1-CHARM (32X SN6.B)	pXRF	Shavings	Bi	0.16	0.16	0.15	0.17	0.02	0.14	0.16	0.02	0.02	0.13	0.03	0.03	18.39	18.83
1-CHARM (32X SN6.B)	pXRF	Shavings	Co	0.8	0.79	0.78	0.81	0.03	0.77	0.82	0.05	0.03	0.75	0.05	0.04	5.58	5.54
1-CHARM (32X SN6.B)	pXRF	Shavings	Cu	85.73	85.73	85.68	85.78	0.1	85.68	85.8	0.12	0.1	85.73	0.08	0.07	0.09	0.08
1-CHARM (32X SN6.B)	pXRF	Shavings	Fe	0.39	0.38	0.36	0.42	0.06	0.35	0.4	0.05	0.06	0.38	0.04	0.02	9.46	6.52
1-CHARM (32X SN6.B)	pXRF	Shavings	Mn	0.11	0.1	0.1	0.12	0.01	0.1	0.12	0.02	0.01	0.09	0.02	0.02	17.12	14.29
1-CHARM (32X SN6.B)	pXRF	Shavings	Ni	0.33	0.33	0.32	0.34	0.03	0.31	0.34	0.03	0.03	0.3	0.04	0.03	10.39	9.51
1-CHARM (32X SN6.B)	pXRF	Shavings	Pb	2.22	2.24	2.19	2.25	0.06	2.17	2.27	0.1	0.07	1.64	0.58	0.6	25.94	26.61
1-CHARM (32X SN6.B)	pXRF	Shavings	Sb	0.27	0.27	0.27	0.28	0.01	0.26	0.28	0.02	0.01	0.3	0.03	0.03	11.47	12.59
1-CHARM (32X SN6.B)	pXRF	Shavings	Sn	7.05	7.09	7	7.11	0.11	7.02	7.14	0.12	0.11	6.78	0.27	0.31	3.83	4.37
1-CHARM (32X SN6.B)	pXRF	Shavings	Zn	1.99	1.98	1.97	2.02	0.05	1.96	2.01	0.05	0.05	2	0.04	0.04	2.13	1.81
1-CHARM (32X SN6.B)	ED-XRF	Shavings	Ag	2.13	2	1.99	2.28	0.29	1.99	2.03	0.03	0.32	1.01	1.12	0.99	51.95	49.7
1-CHARM (32X SN6.B)	ED-XRF	Shavings	As	0.49	0.51	0.46	0.52	0.06	0.5	0.52	0.02	0.06	0.8	0.32	0.29	68.63	57.37
1-CHARM (32X SN6.B)	ED-XRF	Shavings	Bi	0.07	0.08	0.06	0.08	0.02	0.06	0.08	0.02	0.02	0.13	0.06	0.05	125.16	66.67

Appendix. Continuation

Reference	Method	Type	Metal	Mean	Median	95% CI Lower	95% CI Upper	95% CI Length	First quartile	Third quartile	IQR	Standard deviation	Reference value	Mean absolute difference	Median absolute difference	Mean absolute percentage difference	Median absolute percentage difference
1-CHARM (32X SN6.B)	ED-XRF	Shavings	Co	0.75	0.76	0.73	0.76	0.03	0.75	0.76	0.01	0.03	0.75	0.02	0.01	2.5	0.83
1-CHARM (32X SN6.B)	ED-XRF	Shavings	Cu	73.48	74.99	71.68	75.29	3.62	74.9	75.02	0.12	3.97	85.73	12.25	10.74	17.03	14.32
1-CHARM (32X SN6.B)	ED-XRF	Shavings	Fe	0.48	0.49	0.46	0.5	0.05	0.48	0.51	0.03	0.05	0.38	0.11	0.11	20.98	23.14
1-CHARM (32X SN6.B)	ED-XRF	Shavings	Mn	0.09	0.09	0.08	0.1	0.01	0.09	0.09	0	0.01	0.09	0.01	0	9.85	3.37
1-CHARM (32X SN6.B)	ED-XRF	Shavings	Ni	0.32	0.35	0.29	0.34	0.05	0.26	0.35	0.09	0.05	0.3	0.05	0.05	18.02	15.67
1-CHARM (32X SN6.B)	ED-XRF	Shavings	Pb	1.09	1.14	1.02	1.16	0.14	1.14	1.15	0.01	0.15	1.64	0.55	0.5	54.46	43.58
1-CHARM (32X SN6.B)	ED-XRF	Shavings	Sb	0.76	0.7	0.69	0.84	0.16	0.69	0.7	0.01	0.17	0.3	0.46	0.39	58.84	56.32
1-CHARM (32X SN6.B)	ED-XRF	Shavings	Sn	17.76	16.22	16.03	19.5	3.47	16.21	16.33	0.12	3.81	6.78	10.98	9.44	60.62	58.2
1-CHARM (32X SN6.B)	ED-XRF	Shavings	Zn	1.63	1.66	1.6	1.66	0.06	1.65	1.66	0.01	0.07	2	0.37	0.34	23.08	20.85
2-CHARM (31X 78359.B)	pXRF	Shavings	Ag	1.77	1.73	1.72	1.82	0.1	1.71	1.76	0.05	0.1	2.01	0.25	0.28	14.23	16.35
2-CHARM (31X 78359.B)	pXRF	Shavings	As	0	0	0	0	0	0	0	0	0	0.1	0.1	0.1		
2-CHARM (31X 78359.B)	pXRF	Shavings	Bi	1.08	1.1	1.04	1.12	0.08	1.06	1.14	0.08	0.08	0.91	0.17	0.19	15.11	17.23
2-CHARM (31X 78359.B)	pXRF	Shavings	Co	0.13	0.13	0.12	0.13	0.01	0.12	0.13	0.01	0.01	0.11	0.01	0.01	10.39	11
2-CHARM (31X 78359.B)	pXRF	Shavings	Cu	76.75	76.72	76.67	76.82	0.15	76.64	76.82	0.18	0.15	76.6	0.16	0.13	0.21	0.16

Reference	Method	Type	Metal	Mean	Median	95% CI Lower	95% CI Upper	95% CI Length	First quartile	Third quartile	IQR	Standard deviation	Reference value	Mean absolute difference	Median absolute difference	Mean absolute percentage difference	Median absolute percentage difference
2-CHARM (31X 78359.B)	pXRF	Shavings	Fe	0.28	0.29	0.26	0.3	0.04	0.27	0.31	0.03	0.04	0.19	0.09	0.1	30.21	34.58
2-CHARM (31X 78359.B)	pXRF	Shavings	Mn	0	0	0	0	0	0	0	0	0	0	0.01	0		
2-CHARM (31X 78359.B)	pXRF	Shavings	Ni	0.21	0.2	0.2	0.22	0.02	0.2	0.21	0.02	0.02	0.2	0.02	0.01	7.09	5.06
2-CHARM (31X 78359.B)	pXRF	Shavings	Pb	1.41	1.41	1.38	1.45	0.07	1.37	1.46	0.09	0.07	1.04	0.37	0.37	25.86	26.09
2-CHARM (31X 78359.B)	pXRF	Shavings	Sb	0.41	0.4	0.39	0.42	0.03	0.39	0.42	0.03	0.03	0.44	0.04	0.04	9.71	9.05
2-CHARM (31X 78359.B)	pXRF	Shavings	Sn	1.64	1.64	1.63	1.66	0.04	1.63	1.66	0.03	0.04	1.6	0.05	0.04	2.83	2.68
2-CHARM (31X 78359.B)	pXRF	Shavings	Zn	15.9	15.9	15.84	15.95	0.11	15.81	15.99	0.18	0.12	16.26	0.36	0.36	2.29	2.28
2-CHARM (31X 78359.B)	ED-XRF	Shavings	Ag	5.26	4.94	4.86	5.66	0.79	4.87	5.04	0.18	0.9	2.01	3.25	2.93	60.94	59.26
2-CHARM (31X 78359.B)	ED-XRF	Shavings	As	0.06	0.06	0.05	0.06	0.01	0.06	0.07	0.01	0.01	0.1	0.04	0.04	78.74	58.31
2-CHARM (31X 78359.B)	ED-XRF	Shavings	Bi	0.73	0.78	0.69	0.78	0.09	0.71	0.79	0.08	0.1	0.91	0.18	0.13	27.51	16.03
2-CHARM (31X 78359.B)	ED-XRF	Shavings	Co	0.1	0.1	0.1	0.1	0.01	0.1	0.1	0.01	0.01	0.11	0.01	0.01	12.26	13.85

Appendix. Continuation

Reference	Method	Type	Metal	Mean	Median	95% CI Lower	95% CI Upper	95% CI Length	First quartile	Third quartile	IQR	Standard deviation	Reference value	Mean absolute difference	Median absolute difference	Mean absolute percentage difference	Median absolute percentage difference
2-CHARM (31X 78359.B)	ED-XRF	Shavings	Cu	70.91	71.54	70.07	71.75	1.68	71.32	71.74	0.42	1.9	76.6	5.69	5.05	8.11	7.07
2-CHARM (31X 78359.B)	ED-XRF	Shavings	Fe	0.23	0.23	0.22	0.23	0.01	0.22	0.23	0	0.01	0.19	0.04	0.04	15.7	15.93
2-CHARM (31X 78359.B)	ED-XRF	Shavings	Mn	0.01	0.01	0.01	0.01	0	0.01	0.01	0	0	0	0	0	48.45	50.97
2-CHARM (31X 78359.B)	ED-XRF	Shavings	Ni	0.22	0.24	0.2	0.23	0.03	0.18	0.24	0.07	0.04	0.2	0.04	0.05	19.08	18.97
2-CHARM (31X 78359.B)	ED-XRF	Shavings	Pb	0.82	0.86	0.78	0.87	0.09	0.85	0.87	0.02	0.1	1.04	0.22	0.18	29.01	21.05
2-CHARM (31X 78359.B)	ED-XRF	Shavings	Sb	1.31	1.21	1.17	1.45	0.28	1.18	1.23	0.05	0.32	0.44	0.87	0.77	65.3	63.59
2-CHARM (31X 78359.B)	ED-XRF	Shavings	Sn	4.56	4.19	4.08	5.04	0.96	4.09	4.26	0.17	1.08	1.6	2.96	2.59	63.64	61.85
2-CHARM (31X 78359.B)	ED-XRF	Shavings	Zn	14.01	14.05	13.94	14.09	0.15	14.01	14.09	0.08	0.17	16.26	2.25	2.21	16.05	15.73
3-CHARM (31X TB5.B)	pXRF	Shavings	Ag	0.06	0	0.02	0.11	0.09	0	0.21	0.21	0.1	0.22	0.16	0.22		
3-CHARM (31X TB5.B)	pXRF	Shavings	As	0	0	0	0	0	0	0	0	0	0.4	0.4	0.4		
3-CHARM (31X TB5.B)	pXRF	Shavings	Bi	0.38	0.38	0.37	0.39	0.03	0.37	0.4	0.03	0.03	0.29	0.09	0.08	22.63	22.34

Reference	Method	Type	Metal	Mean	Median	95% CI Lower	95% CI Upper	95% CI Length	First quartile	Third quartile	IQR	Standard deviation	Reference value	Mean absolute difference	Median absolute difference	Mean absolute percentage difference	Median absolute percentage difference
3-CHARM (31X TB5.B)	pXRF	Shavings	Co	0.01	0	0	0.02	0.01	0	0.02	0.02	0.01	0.02	0.01	0.02		
3-CHARM (31X TB5.B)	pXRF	Shavings	Cu	61.24	61.2	61.17	61.31	0.14	61.12	61.39	0.27	0.16	61.49	0.25	0.3	0.41	0.48
3-CHARM (31X TB5.B)	pXRF	Shavings	Fe	0.08	0.09	0.08	0.09	0.01	0.08	0.1	0.02	0.01	0.09	0.01	0.01	16.14	9.3
3-CHARM (31X TB5.B)	pXRF	Shavings	Mn	0.31	0.31	0.3	0.32	0.02	0.3	0.32	0.02	0.02	0.28	0.03	0.03	9.06	8.71
3-CHARM (31X TB5.B)	pXRF	Shavings	Ni	0.11	0.11	0.11	0.12	0.01	0.11	0.12	0.01	0.01	0.11	0.01	0.01	8.28	7.02
3-CHARM (31X TB5.B)	pXRF	Shavings	Pb	0.78	0.77	0.75	0.8	0.05	0.74	0.78	0.04	0.05	0.57	0.2	0.19	25.68	24.93
3-CHARM (31X TB5.B)	pXRF	Shavings	Sb	0.23	0.22	0.22	0.23	0.02	0.21	0.24	0.03	0.02	0.23	0.02	0.02	7.82	9.13
3-CHARM (31X TB5.B)	pXRF	Shavings	Sn	0.14	0.15	0.14	0.15	0.01	0.14	0.15	0.01	0.01	0.13	0.02	0.02	12.43	13.42
3-CHARM (31X TB5.B)	pXRF	Shavings	Zn	36.16	36.23	36.07	36.26	0.19	36.09	36.31	0.21	0.2	35.62	0.54	0.61	1.5	1.69
3-CHARM (31X TB5.B)	ED-XRF	Shavings	Ag	0.66	0.6	0.58	0.74	0.15	0.59	0.61	0.01	0.17	0.22	0.45	0.38	65.94	64
3-CHARM (31X TB5.B)	ED-XRF	Shavings	As	0.31	0.33	0.29	0.33	0.04	0.32	0.33	0.01	0.04	0.4	0.08	0.07	30.83	20.82
3-CHARM (31X TB5.B)	ED-XRF	Shavings	Bi	0.27	0.28	0.25	0.29	0.04	0.28	0.29	0	0.04	0.29	0.02	0.01	12.77	2.93
3-CHARM (31X TB5.B)	ED-XRF	Shavings	Co	0.01	0	0	0.01	0.01	0	0.01	0.01	0.01	0.02	0.01	0.02	1450.78	531.87
3-CHARM (31X TB5.B)	ED-XRF	Shavings	Cu	59.42	59.96	58.65	60.19	1.53	59.9	60.08	0.17	1.73	61.49	2.07	1.53	3.57	2.54
3-CHARM (31X TB5.B)	ED-XRF	Shavings	Fe	0.11	0.1	0.1	0.11	0.01	0.1	0.11	0	0.01	0.09	0.01	0.01	11.54	9.31
3-CHARM (31X TB5.B)	ED-XRF	Shavings	Mn	0.25	0.26	0.23	0.28	0.05	0.23	0.28	0.05	0.05	0.28	0.04	0.03	25.7	11.9

Appendix. Continuation

Reference	Method	Type	Metal	Mean	Median	95% CI Lower	95% CI Upper	95% CI Length	First quartile	Third quartile	IQR	Standard deviation	Reference value	Mean absolute difference	Median absolute difference	Mean absolute percentage difference	Median absolute percentage difference
3-CHARM (31X TB5.B)	ED-XRF	Shavings	Ni	0.13	0.14	0.12	0.14	0.02	0.11	0.14	0.03	0.02	0.11	0.03	0.04	20.13	25.19
3-CHARM (31X TB5.B)	ED-XRF	Shavings	Pb	0.5	0.51	0.47	0.53	0.06	0.51	0.52	0.01	0.07	0.57	0.08	0.06	18.61	12.61
3-CHARM (31X TB5.B)	ED-XRF	Shavings	Sb	0.89	0.76	0.73	1.06	0.33	0.75	0.76	0.01	0.37	0.23	0.66	0.53	72.02	69.92
3-CHARM (31X TB5.B)	ED-XRF	Shavings	Sn	0.49	0.41	0.4	0.57	0.18	0.41	0.42	0.01	0.2	0.13	0.36	0.28	71.15	68.81
3-CHARM (31X TB5.B)	ED-XRF	Shavings	Zn	33.52	33.51	33.4	33.64	0.24	33.49	33.54	0.05	0.27	35.62	2.1	2.11	6.28	6.3
8-CHARM (33X GM21.B)	pXRF	Shavings	Ag	0.64	0.62	0.62	0.67	0.05	0.61	0.71	0.1	0.05	0.7	0.07	0.08	11.64	13.25
8-CHARM (33X GM21.B)	pXRF	Shavings	As	0	0	0	0	0	0	0	0	0	0.33	0.33	0.33		
8-CHARM (33X GM21.B)	pXRF	Shavings	Bi	0.59	0.6	0.56	0.62	0.05	0.54	0.63	0.09	0.06	0.46	0.13	0.14	21.43	23.24
8-CHARM (33X GM21.B)	pXRF	Shavings	Co	0.13	0.13	0.13	0.14	0.01	0.13	0.14	0.01	0.01	0	0.13	0.13	100	100
8-CHARM (33X GM21.B)	pXRF	Shavings	Cu	76.92	76.86	76.82	77.02	0.2	76.78	77	0.22	0.22	78.86	1.94	2	2.52	2.6
8-CHARM (33X GM21.B)	pXRF	Shavings	Fe	0.63	0.61	0.6	0.66	0.06	0.58	0.7	0.11	0.07	0.69	0.08	0.08	13.46	13.42
8-CHARM (33X GM21.B)	pXRF	Shavings	Mn	0.05	0.07	0.03	0.07	0.03	0	0.08	0.08	0.04	0	0.05	0.07	100	100

Reference	Method	Type	Metal	Mean	Median	95% CI Lower	95% CI Upper	95% CI Length	First quartile	Third quartile	IQR	Standard deviation	Reference value	Mean absolute difference	Median absolute difference	Mean absolute percentage difference	Median absolute percentage difference
8-CHARM (33X GM21.B)	pXRF	Shavings	Ni	0.19	0.19	0.18	0.2	0.02	0.18	0.2	0.02	0.02	0.2	0.01	0.01	7.19	4.23
8-CHARM (33X GM21.B)	pXRF	Shavings	Pb	10.11	10.21	9.98	10.23	0.25	9.84	10.28	0.45	0.27	7.53	2.58	2.68	25.43	26.23
8-CHARM (33X GM21.B)	pXRF	Shavings	Sb	0.96	0.93	0.93	0.98	0.05	0.92	1.03	0.11	0.06	1.03	0.08	0.1	8.64	11.08
8-CHARM (33X GM21.B)	pXRF	Shavings	Sn	4.55	4.52	4.49	4.6	0.11	4.47	4.6	0.12	0.12	4.5	0.09	0.06	1.88	1.36
8-CHARM (33X GM21.B)	pXRF	Shavings	Zn	4.76	4.75	4.73	4.79	0.05	4.72	4.8	0.08	0.06	4.96	0.2	0.21	4.23	4.4
8-CHARM (33X GM21.B)	ED-XRF	Shavings	Ag	1.63	1.52	1.53	1.73	0.21	1.52	1.55	0.03	0.24	0.7	0.93	0.82	56.32	53.97
8-CHARM (33X GM21.B)	ED-XRF	Shavings	As	0.2	0.21	0.19	0.2	0.02	0.19	0.21	0.02	0.02	0.33	0.14	0.13	70.48	61.18
8-CHARM (33X GM21.B)	ED-XRF	Shavings	Bi	0.38	0.42	0.35	0.41	0.06	0.33	0.42	0.09	0.06	0.46	0.08	0.04	24.93	8.9
8-CHARM (33X GM21.B)	ED-XRF	Shavings	Co	0.1	0.09	0.1	0.1	0.01	0.09	0.1	0.01	0.01	0	0.1	0.09	100	100
8-CHARM (33X GM21.B)	ED-XRF	Shavings	Cu	70.45	71.19	69.58	71.32	1.74	71.12	71.26	0.14	2.01	78.86	8.41	7.67	12.03	10.77
8-CHARM (33X GM21.B)	ED-XRF	Shavings	Fe	0.71	0.73	0.69	0.73	0.04	0.72	0.73	0.01	0.04	0.69	0.04	0.04	6.4	4.98

Appendix. Continuation

Reference	Method	Type	Metal	Mean	Median	95% CI Lower	95% CI Upper	95% CI Length	First quartile	Third quartile	IQR	Standard deviation	Reference value	Mean absolute difference	Median absolute difference	Mean absolute percentage difference	Median absolute percentage difference
8-CHARM (33X GM21.B)	ED-XRF	Shavings	Mn	0.07	0.07	0.06	0.07	0.01	0.06	0.07	0.01	0.01	0	0.07	0.07	100	100
8-CHARM (33X GM21.B)	ED-XRF	Shavings	Ni	0.21	0.24	0.19	0.23	0.04	0.15	0.24	0.09	0.05	0.2	0.05	0.05	23.28	19.16
8-CHARM (33X GM21.B)	ED-XRF	Shavings	Pb	6.11	6.56	5.77	6.46	0.69	6.01	6.56	0.55	0.8	7.53	1.42	0.97	25.77	14.82
8-CHARM (33X GM21.B)	ED-XRF	Shavings	Sb	2.76	2.51	2.52	3	0.49	2.49	2.54	0.04	0.56	1.03	1.73	1.48	61.45	58.84
8-CHARM (33X GM21.B)	ED-XRF	Shavings	Sn	11.6	10.54	10.6	12.59	1.99	10.5	10.74	0.25	2.3	4.5	7.1	6.04	60.08	57.31
8-CHARM (33X GM21.B)	ED-XRF	Shavings	Zn	4.18	4.2	4.15	4.21	0.06	4.19	4.21	0.02	0.07	4.96	0.78	0.76	18.69	18.24
9-CHARM (32X LB10.G)	pXRF	Shavings	Ag	0	0	0	0	0	0	0	0	0	0.07	0.07	0.07		
9-CHARM (32X LB10.G)	pXRF	Shavings	As	0	0	0	0	0	0	0	0	0	0.17	0.17	0.17		
9-CHARM (32X LB10.G)	pXRF	Shavings	Bi	0.1	0.12	0.07	0.13	0.07	0.02	0.14	0.12	0.07	0.09	0.06	0.06		37.48
9-CHARM (32X LB10.G)	pXRF	Shavings	Co	0.1	0.1	0.09	0.11	0.01	0.09	0.11	0.02	0.01	0.08	0.02	0.02	17.12	17.65
9-CHARM (32X LB10.G)	pXRF	Shavings	Cu	73.66	73.65	73.57	73.74	0.16	73.58	73.76	0.18	0.17	77.1	3.44	3.45	4.68	4.69

Reference	Method	Type	Metal	Mean	Median	95% CI Lower	95% CI Upper	95% CI Length	First quartile	Third quartile	IQR	Standard deviation	Reference value	Mean absolute difference	Median absolute difference	Mean absolute percentage difference	Median absolute percentage difference
9-CHARM (32X LB10.G)	pXRF	Shavings	Fe	0.04	0	0.01	0.08	0.08	0	0.09	0.09	0.08	0	0.05	0		
9-CHARM (32X LB10.G)	pXRF	Shavings	Mn	0	0	0	0	0	0	0	0	0	0	0	0		
9-CHARM (32X LB10.G)	pXRF	Shavings	Ni	0.68	0.68	0.67	0.69	0.02	0.67	0.69	0.02	0.02	0.69	0.02	0.02	3.05	2.37
9-CHARM (32X LB10.G)	pXRF	Shavings	Pb	16.33	16.33	16.25	16.41	0.16	16.22	16.45	0.24	0.16	12.6	3.73	3.73	22.84	22.86
9-CHARM (32X LB10.G)	pXRF	Shavings	Sb	0.55	0.54	0.53	0.56	0.03	0.53	0.55	0.02	0.03	0.6	0.05	0.06	9.89	11.24
9-CHARM (32X LB10.G)	pXRF	Shavings	Sn	8.34	8.35	8.29	8.39	0.1	8.27	8.42	0.15	0.1	8.29	0.09	0.07	1.1	0.91
9-CHARM (32X LB10.G)	pXRF	Shavings	Zn	0.05	0	0.02	0.08	0.06	0	0.12	0.12	0.06	0.11	0.07	0.11		
9-CHARM (32X LB10.G)	ED-XRF	Shavings	Ag	0.14	0.14	0.14	0.15	0.02	0.13	0.14	0.01	0.02	0.07	0.07	0.07	51.54	50.51
9-CHARM (32X LB10.G)	ED-XRF	Shavings	As	0.04	0.05	0.04	0.05	0.01	0.04	0.05	0.01	0.01	0.17	0.13	0.12	433.25	247.74
9-CHARM (32X LB10.G)	ED-XRF	Shavings	Bi	0.06	0.07	0.05	0.07	0.02	0.04	0.07	0.03	0.02	0.09	0.04	0.02	154.01	35.17
9-CHARM (32X LB10.G)	ED-XRF	Shavings	Co	0.07	0.06	0.06	0.07	0.01	0.06	0.07	0.01	0.01	0.08	0.02	0.02	29.99	38.16

Appendix. Continuation

Reference	Method	Type	Metal	Mean	Median	95% CI Lower	95% CI Upper	95% CI Length	First quartile	Third quartile	IQR	Standard deviation	Reference value	Mean absolute difference	Median absolute difference	Mean absolute percentage difference	Median absolute percentage difference
9-CHARM (32X LB10.G)	ED-XRF	Shavings	Cu	64.29	66.27	62.26	66.32	4.06	66.08	66.34	0.26	4.69	77.1	12.81	10.83	20.62	16.34
9-CHARM (32X LB10.G)	ED-XRF	Shavings	Fe	0.02	0.01	0.01	0.03	0.02	0.01	0.02	0.02	0.02	0	0.02	0.01	88.07	88.17
9-CHARM (32X LB10.G)	ED-XRF	Shavings	Mn	0	0	0	0	0	0	0	0	0	0	0	0	100	100
9-CHARM (32X LB10.G)	ED-XRF	Shavings	Ni	0.6	0.64	0.57	0.63	0.06	0.56	0.65	0.09	0.07	0.69	0.09	0.05	17.29	7.29
9-CHARM (32X LB10.G)	ED-XRF	Shavings	Pb	8.89	9.54	8.25	9.52	1.27	9.37	9.57	0.21	1.47	12.6	3.71	3.06	47.12	32.02
9-CHARM (32X LB10.G)	ED-XRF	Shavings	Sb	1.66	1.46	1.46	1.85	0.39	1.45	1.48	0.02	0.45	0.6	1.06	0.87	61.99	59.11
9-CHARM (32X LB10.G)	ED-XRF	Shavings	Sn	22.97	20.58	20.54	25.4	4.85	20.48	20.64	0.16	5.61	8.29	14.68	12.29	62.38	59.72
9-CHARM (32X LB10.G)	ED-XRF	Shavings	Zn	0.12	0.1	0.11	0.14	0.04	0.09	0.17	0.08	0.04	0.11	0.04	0.03	28.18	34.99